



Published in final edited form as:

*J Cardiovasc Pharmacol.* 2013 July ; 62(1): 26–40. doi:10.1097/FJC.0b013e31828bc88a.

## Subtype-Specific Estrogen Receptor-Mediated Vasodilator Activity in the Cephalic, Thoracic and Abdominal Vasculature of Female Rat

Ossama M. Reslan, Zongzhi Yin, Graciliano R. A. do Nascimento, and Raouf A. Khalil

Vascular Surgery Research Laboratory, Division of Vascular and Endovascular Surgery, Brigham and Women's Hospital, and Harvard Medical School, Boston, MA

### Abstract

Estrogen receptors (ERs) mediate genomic and nongenomic vasodilator effects, but estrogen therapy may not provide systemic vascular protection. To test whether this is due to regional differences in ER distribution or vasodilator activity, cephalic (carotid), thoracic (thoracic aorta, pulmonary) and abdominal arteries (abdominal aorta, mesenteric, renal) from female Sprague-Dawley rats were prepared to measure contraction to phenylephrine (Phe), and relaxation to acetylcholine (ACh) and the ER activators 17 $\beta$ -estradiol (E2) (all ERs), PPT (ER $\alpha$ ), DPN (ER $\beta$ ) and G1 (GPR30). Phe caused contraction that was enhanced in endothelium-denuded aorta, supporting endothelial release of vasodilators. In cephalic and thoracic arteries, ACh relaxation was abolished by the NOS inhibitor L-NAME, suggesting a role of NO. In mesenteric vessels, ACh-induced relaxation was partly inhibited by L-NAME+COX inhibitor indomethacin and blocked by the K<sup>+</sup> channel blocker tetraethylammonium (TEA), suggesting a hyperpolarization pathway. E2 and PPT caused similar relaxation in all vessels. DPN and G1 caused smaller relaxation that was more prominent in abdominal vessels. RT-PCR revealed variable ER $\alpha$  mRNA expression, and increased ER $\beta$  in carotid artery and GPR30 in abdominal arteries. Western blots revealed greater amounts of ER $\alpha$ , ER $\beta$  and GPR30 in abdominal arteries. In thoracic aorta, E2, PPT and DPN-induced relaxation was blocked by L-NAME, and was associated with increased nitrite/nitrate production, suggesting a role of NO. In abdominal vessels, E2, PPT, DPN and G1-induced relaxation persisted in L-NAME+indomethacin+TEA-treated or endothelium-denuded arteries, suggesting direct effect on vascular smooth muscle (VSM). E2, PPT, DPN, and G1 caused greater relaxation of KCl-induced contraction in abdominal vessels, suggesting inhibitory effects on Ca<sup>2+</sup> entry. Thus, E2 and ER $\alpha$  stimulation produce similar relaxation of the cephalic, thoracic and abdominal arteries. In the cephalic and thoracic arteries, particularly the thoracic aorta, E2-induced and ER $\alpha$ - and ER $\beta$ -mediated vasodilation involve NO production. ER $\beta$ - and GPR30-mediated relaxation is greater in the abdominal arteries, and appears to involve hyperpolarization and inhibition of VSM Ca<sup>2+</sup> entry. Specific ER agonists could produce vasodilation in specific vascular beds without affecting other vessels in systemic circulation.

### Keywords

estrogen; sex hormones; endothelium; vascular smooth muscle

## INTRODUCTION

Cardiovascular disease is less common in premenopausal women than in men of similar age or postmenopausal women, suggesting vascular protective effects of estrogen (E2).<sup>1-5</sup> Experimental studies have also shown sex differences in vasoconstriction, and supported vascular benefits of E2 in females.<sup>6-10</sup> The beneficial effects of E2 have been ascribed to modification of circulating lipoproteins,<sup>2, 11</sup> changes in blood coagulation,<sup>12</sup> inhibition of intravascular accumulation of collagen,<sup>13</sup> and both genomic and non-genomic effects on blood vessels.<sup>4, 14, 15</sup> Genomic effects of E2 include stimulation of endothelial cell growth,<sup>3, 4</sup> upregulation of endothelial nitric oxide (NO) synthase and NO production and the cyclooxygenase (COX) pathway and prostacyclin (PGI<sub>2</sub>) production,<sup>4, 14</sup> as well as inhibition of vascular smooth muscle (VSM) proliferation and downregulation of VSM Ca<sup>2+</sup> channels and protein kinase C.<sup>7, 16</sup> E2 also causes rapid nongenomic vasodilation via activation of endothelium-dependent NO, PGI<sub>2</sub> and hyperpolarization pathways,<sup>17, 18</sup> and inhibition of Ca<sup>2+</sup>-dependent mechanisms of VSM contraction.<sup>4, 10, 19</sup>

Many of the effects of E2 are mediated via estrogen receptors (ERs).<sup>20</sup> ERs have been identified in the female reproductive tract, mammary glands, and other tissues, as well as in blood vessels of experimental animals and humans.<sup>20-23</sup> ER $\alpha$  and ER $\beta$  mediate many of the genomic effects of E2,<sup>20, 22, 23</sup> and surface membrane ER $\alpha$  and ER $\beta$  have been implicated in the rapid vasodilator effects of E2.<sup>15</sup> A transmembrane G protein-coupled receptor GPR30 may also bind E2 and mediate some of its rapid effects.<sup>24-28</sup> Although several studies support vasodilator effects of E2, estrogenic hormone therapy has not produced significant vascular protection.<sup>3, 14</sup> This could be partly related to the patient's age, preexisting cardiovascular condition, and the estrogen dose, formulation, and route of administration.<sup>3, 14, 20</sup> The lack of systemic vascular protection by estrogenic hormone therapy could also be related to differential effects of E2 on different vascular beds due to regional differences in the distribution/activity of vascular ERs. In this respect, a vasodilator effect of E2 in one vascular bed could be masked by the lack of effect or minimal effect in other vascular beds, resulting in an overall little systemic vasodilator effect. Previous studies have examined the sex differences and the effects of E2 on vascular function,<sup>4, 10, 15, 17-19</sup> and ER $\alpha$ , ER $\beta$  and GPR30 have been identified in blood vessels of human and experimental animals.<sup>21-23, 29-31</sup> However, the regional differences in the expression/activity of vascular ER subtypes have not been clearly examined. In some instances, studies have used one vascular bed as a prototype to study the effects of E2 on vascular function; however, findings in one blood vessel cannot always be generalized to other vessels in the systemic circulation. Also, the diverse results from separate studies describing the role of one ER subtype in one vascular bed have made it difficult to compare the role of different ER subtypes on vascular function in different vascular beds. Furthermore, because vascular pathology can be localized to certain vascular beds, understanding the regional differences in vascular ER expression/activity should help design more specific estrogenic therapy and drug targeting approaches for localized vascular disease.

The purpose of this study was to test the hypothesis that vascular ER subtypes exhibit regional differences in their expression/vasodilator activity. We used three blood vessels from the cephalic and thoracic circulation, three blood vessels from the abdominal circulation of female rat, and three subtype-specific ER agonists to test whether: 1) ER-mediated vasodilation is both ER agonist- and blood vessel-specific, 2) the differences in ER-mediated vasodilation reflect regional differences in the expression of vascular ERs, and 3) the differences in ER-mediated vasodilation reflect regional differences in the post-ER-mediated endothelium-dependent vascular relaxation pathways and/or endothelium-independent inhibitory effects on VSM contraction mechanisms.

## METHODS

### Animals and Tissues

Female Sprague-Dawley rats (12 wk, 250-300g, Charles River lab, Wilmington, MA) were maintained on *ad libitum* standard rat chow and tap water in 12 hr/12 hr light/dark cycle. Because vascular reactivity can be influenced by sex hormones during the estrus cycle, all experiments were conducted in female rats during estrus, in order to control for endocrine confounders. The estrus cycle was determined by taking a vaginal smear with a pasteur pipette.<sup>32</sup> An estrus smear primarily contained anucleated cornified squamous cells<sup>33</sup> and was confirmed prior to all experiments. Rats were euthanized by inhalation of CO<sub>2</sub>. The thoracic cavity and neck region were opened and the thoracic aorta, right and left carotid artery, and right and left pulmonary artery were excised. The abdominal cavity was also opened and the abdominal aorta, second branch mesenteric arteries, and right and left renal artery were excised. The arteries were placed in oxygenated Krebs solution, and carefully dissected and cleaned of connective tissue under microscopic visualization. The arteries were portioned into 3-mm wide rings in preparation for isometric contraction experiments. For endothelium-intact arterial segments extreme care was taken throughout the tissue isolation and dissection procedure in order to minimize injury to the endothelium. For endothelium-denuded aortic and pulmonary arterial segments, the endothelium was removed by scraping the vessel interior five times around the tip of forceps. For endothelium-denuded carotid, mesenteric and renal artery, the vessel interior was scraped five times around thin tungsten wire. Different vessels were used for different experimental protocols and pharmacological manipulations. All procedures followed the NIH Guide for the Care and Use of Laboratory Animals, and approved protocols by the Harvard Medical Area Standing Committee on Animals at Harvard Medical School.

### Isometric Contraction

Circular vascular segments were suspended between two stainless-steel hooks, one hook was fixed at the bottom of a tissue bath and the other hook was connected to a Grass force displacement transducer (FT03, Astro-Med Inc., West Warwick, RI). Arterial segments were stretched under 2 g (thoracic and abdominal aorta), 1 g (carotid and pulmonary artery), or 0.5 g basal tension (mesenteric and renal artery) and allowed to equilibrate for 45 min in a tissue bath filled with 50 ml Krebs solution continuously bubbled with 95% O<sub>2</sub> 5% CO<sub>2</sub> at 37 °C. Preliminary experiments to construct the relationship between basal tension and the contraction to 96 mM KCl demonstrated that these basal tensions produced maximal KCl contraction, and further increases in basal tension did not cause any significant increases in the contractile response to KCl. The changes in isometric contraction/relaxation were recorded on a Grass polygraph (Model 7D, Astro-Med Inc.).

Control contraction in response to 96 mM KCl was first elicited. Once the KCl maximum contraction was reached and a plateau achieved (within 10 to 15 min) the tissue was washed 3 times in Krebs, 10 min each. The control contraction to 96 mM KCl was repeated twice prior to further experimentation. Vascular segments were then stimulated with increasing concentrations (10<sup>-9</sup> to 10<sup>-5</sup> M) of phenylephrine (Phe), and the contractile response was measured. To correct for differences in the arterial segment size, all contraction measurements were normalized to the weight of the arterial segments and presented as g/mg tissue weight. The contractile response at each Phe concentration was also presented as % of maximum Phe contraction. The individual Phe concentration-response curves were analyzed using a non-linear regression curve (best-fit sigmoidal dose-response curve, Sigmaplot), and the effective concentration that produced half the maximal contraction (EC<sub>50</sub>) was presented as pEC<sub>50</sub> (-log M).

To investigate the endothelial function, vascular segments precontracted with Phe were treated with acetylcholine (ACh,  $10^{-9}$  to  $10^{-5}$  M), the % relaxation was measured and concentration-relaxation curve to ACh were constructed. Although extreme care was taken throughout the procedure to minimize injury to the endothelium, the magnitude of the ACh relaxation varied, suggesting variable degrees of endothelium integrity among the vessels tested. However, none of the vessels tested showed complete relaxation to ACh (completely intact endothelium) or lack of relaxation to ACh (total damage of the endothelium). No exclusion criteria were implemented, and all ACh concentration-relaxation data were included in the analysis. To test the role of ERs, vascular segments precontracted with Phe were treated with increasing concentrations ( $10^{-12}$  to  $10^{-5}$  M) of  $17\beta$ -estradiol (E2, activator of all ERs), 4,4',4''-(4-propyl-[1H]-pyrazole-1,3,5-triyl)-tris-phenol (PPT, selective ER $\alpha$  agonist),<sup>34, 35</sup> diarylpropionitrile (DPN, selective ER $\beta$  agonist),<sup>36</sup> or ( $\pm$ )-1-[(3aR\*,4S\*,9bS\*)-4-(6-Bromo-1,3-benzodioxol-5-yl)-3a,4,5,9b-tetrahydro-3H-cyclopenta[c]quinolin-8-yl]-ethanone (G1, GPR30 agonist),<sup>37, 38</sup> and the % vascular relaxation was measured. For construction of concentration-response curves, each ER agonist concentration was added and the vascular response was observed until it reached steady-state or for 10 min whichever happened first, then the next concentration was added. To test the specificity of the effects of E2, PPT, DPN and G1, control experiments were performed to examine the effects of the vehicle ethanol (0.1%, for E2) and DMSO (0.1%, for PPT, DPN and G1). In other control experiments, the effects of PPT, DPN and G1 were examined in vessels pretreated with the ER $\alpha$  antagonist MPP (1,3-Bis(4-hydroxyphenyl)-4-methyl-5-[4-(2-piperidinyloxy)phenol]-1H-pyrazole), ER $\beta$  antagonist PHTPP (4-[2-Phenyl-5,7-bis(trifluoromethyl)pyrazolo[1,5-a]pyrimidin-3-yl]phenol), and GPR30 antagonist G15 (3aS\*,4R\*,9bR\*)-4-(6-Bromo-1,3-benzodioxol-5-yl)-3a,4,5,9b-3H-cyclopenta[c]quinoline), respectively.

To test the role of endothelium-dependent NO, PGI<sub>2</sub> and hyperpolarization factor, vascular relaxation was measured in arterial segments treated with the NOS inhibitor N $\omega$ -nitro-L-arginine methyl ester (L-NAME,  $3 \times 10^{-4}$  M), COX inhibitor indomethacin ( $10^{-5}$  M), and tetraethylammonium (TEA, 30 mM), blocker of large conductance Ca<sup>2+</sup>-dependent K<sup>+</sup> channels (BK<sub>Ca</sub>) and hyperpolarization pathway. To test for endothelium-independent effects on VSM, the effects of ER agonists were measured in endothelium-denuded arteries precontracted with Phe. Also, membrane depolarization by high KCl is known to activate Ca<sup>2+</sup> entry through Ca<sup>2+</sup> channels into VSM.<sup>7, 39</sup> To test for ER-mediated effects on Ca<sup>2+</sup> entry into VSM, the effects of ER agonists were tested on endothelium-denuded arteries precontracted with 96 mM KCl.

### Nitrite/Nitrate (NOx) Measurement

Endothelium-intact thoracic aortic segments were placed in 2 ml Krebs aerated with 95% O<sub>2</sub> 5% CO<sub>2</sub> at 37°C for 30 min, and samples for basal accumulation of nitrite (NO<sub>2</sub><sup>-</sup>) formed from released NO were taken. Aortic segments were treated with ACh, E2, PPT, DPN or G1 ( $10^{-5}$  M) for 10 min, then rapidly removed, dabbed dry with filter paper and weighed. The incubation solutions were assayed for the stable end product of NO, NO<sub>2</sub><sup>-</sup>. Briefly, samples of incubation solution (50  $\mu$ l, in triplicate) were mixed in 96-well microplate with 100  $\mu$ l Griess reagent. The chromophore generated from the reaction with NO<sub>2</sub><sup>-</sup> was detected spectrophotometrically (535 nm) using SpectraMAX microplate reader (Molecular Devices, Sunnyvale CA). The concentration of NO<sub>2</sub><sup>-</sup> was calculated using a calibration curve with known concentrations of NaNO<sub>2</sub>.<sup>40</sup>

### Real-Time RT-PCR Analysis

RNA was isolated from arterial rings using RNeasy Fibrous Tissue Mini Kit (QIAGEN, Valencia, CA). 1  $\mu$ g of total RNA was used for reverse transcription to synthesize single-

strand cDNA in a 20  $\mu$ l-reaction mixture according to the protocol of First-Strand cDNA Synthesis Kit (Amersham Biosciences, Pittsburgh, PA). 2  $\mu$ l of cDNA dilution (1:5 for ER $\alpha$ , ER $\beta$  and GPR30, and 1:25 for  $\alpha$ -actin) of reverse transcription (RT) product was applied to 20  $\mu$ l RT-PCR reaction. Quantification of gene expression was performed using real-time quantitative RT-PCR machine (Mx4000 Multiplex Quantitative PCR System, Stratagene, La Jolla, CA) and employing published oligonucleotide primers specific for ER $\alpha$ , ER $\beta$  and GPR30 (Integrated DNA Technologies (IDT), Coralville, IA), and the Bio-Rad iQ SYBR Green Supermix for amplicon detection (Bio-Rad, Hercules, CA).  $\alpha$ -Actin primer was included in the RT-PCR reaction as internal standard to normalize the results.

Primers	Sequences
ER $\alpha$	Forward 5'-AATTCTGACAATCGACGCCAG-3'
	Reverse 5'-GTGCTTCAACATTCTCCCTCCTC-3'
ER $\beta$	Forward 5'-AAAGCCAAGAGAAACGGTGGGCAT-3'
	Reverse 5'-GCCAATCATGTGCACCAGTTCCTT-3'
GPR30	Forward 5'-GCAGCGTCTTCTCCTCACC-3'
	Reverse 5'-ACAGCCTGAGCTTGCCCTG-3'
$\alpha$ -actin	Forward 5'-GACACCAGGGAGTGATGGTT-3'
	Reverse 5'-GTTAGCAAGGTCGGATGCTC-3'

PCR was carried out with 1 cycle for 10 min at 95°C then 40-45 cycles of 30 sec denaturation at 95°C, 45 sec of annealing at 56°C, and 30 sec of extension at 72°C, followed by 1 min of final extension step at 95°C. The number of PCR cycles varies according to the expression level of the target gene. An appropriate primer concentration and number of cycles was determined to ensure that the PCR is taking place in the linear range and thereby guarantees a proportional relationship between input RNA and the cycles readout. The relative gene expression was calculated by comparing cycle thresholds with the housekeeping gene  $\alpha$ -actin.<sup>31</sup> The Ct value for actin was not significantly different between the thoracic aorta (15.93 $\pm$ 0.47), carotid (15.74 $\pm$ 0.56), pulmonary (15.90 $\pm$ 0.49), abdominal aorta (17.15 $\pm$ 0.52), mesenteric (16.42 $\pm$ 0.60) and renal artery (17.07 $\pm$ 0.41).

### Western Blot Analysis

Vascular tissues were homogenized in a buffer containing 20 mM 3-[N-morpholino]propane sulfonic acid, 4% SDS, 10% glycerol, 2.3 mg dithiothreitol, 1.2 mM EDTA, 0.02% BSA, 5.5  $\mu$ M leupeptin, 5.5  $\mu$ M pepstatin, 2.15  $\mu$ M aprotinin and 20  $\mu$ M 4-(2-aminoethyl)-benzenesulfonyl fluoride, using a 2 ml tight-fitting homogenizer (Kontes Glass). The homogenate was centrifuged at 10,000g for 2 min, the supernatant was collected, and the protein concentration was determined using a protein assay kit (Bio-Rad).

Vascular tissue homogenate was subjected to electrophoresis on 8% SDS polyacrylamide gel then transferred electrophoretically to nitrocellulose membrane. The membrane was incubated in 5% dried non-fat milk for 1 hr, then treated with polyclonal antibody to ER $\alpha$ , (1:500), ER $\beta$  (1:1000) and GPR30 (1:500) (Affinity Bioreagents, Golden, CO) for 24 hr. Preliminary Western blots experiments using the same antibody titer for ER $\alpha$ , ER $\beta$  and GPR30 demonstrated prominent immunoreactivity in tissue homogenate of the ovary.  $\alpha$ -Actin was used as an internal control and detected by a monoclonal anti-actin antibody (1:500000, Sigma). The nitrocellulose membranes were washed 5 times for 15 min each in TBS-Tween then incubated in horseradish peroxidase-conjugated secondary antibody (1:1000) for 1.5 hr. The blots were visualized with Enhanced Chemi-Luminescence (ECL)

Western Blotting Detection Reagent (GE Healthcare Bio-Sciences, Piscataway, NJ) and the reactive bands were analyzed quantitatively by optical densitometry. The densitometry values represented the pixel intensity, and were normalized to  $\alpha$ -actin to correct for loading.<sup>29, 31</sup>

### Solutions, Drugs and Chemicals

Normal Krebs solution contained (in mM): 120 NaCl, 5.9 KCl, 25 NaHCO<sub>3</sub>, 1.2 NaH<sub>2</sub>PO<sub>4</sub>, 11.5 dextrose, 2.5 CaCl<sub>2</sub>, and 1.2 MgCl<sub>2</sub>. Krebs solution was bubbled with 95% O<sub>2</sub> and 5% CO<sub>2</sub> for 30 min, at an adjusted pH 7.4. The high KCl (96 mM) or TEA solution (30 mM) was prepared as normal Krebs but with equimolar substitution of NaCl with KCl or TEA, respectively. Stock solutions of Phe (10<sup>-1</sup> M), ACh (10<sup>-1</sup> M), L-NAME (10<sup>-1</sup> M) (Sigma) were prepared in deionized water, 17 $\beta$ -estradiol (E2, 10<sup>-2</sup> M, sigma) in 100% ethanol, and PPT, DPN, G1, ER $\alpha$  antagonist MPP, ER $\beta$  antagonist PHTPP, GPR30 antagonist G15 (10<sup>-1</sup> M, Tocris, Ellisville, MO), and indomethacin (10<sup>-1</sup> M, Sigma) were prepared in dimethylsulfoxide (DMSO). The final concentration of ethanol or DMSO in the experimental solution was <0.1%. All other chemicals were of reagent grade or better.

### Statistical Analysis

The Phe contraction and ACh relaxation experiments were conducted on 2 to 4 vascular segments from each vascular bed from each rat, and the data from different vascular segments were averaged for each rat. The ER agonists experiments were conducted on one vascular segment from each vascular bed from each rat. For the RT-PCR and Western blot experiments, 2 to 4 vascular segments from each vascular bed from each rat were pooled as one sample. Cumulative data from 8 to 10 different rats were presented as means $\pm$ SEM, with the "n" value representing the number of rats. Data were first analyzed using one way ANOVA with Scheffe's F test, where  $F = (\text{variance between groups} / \text{variance within groups})$ . When a statistical difference was observed, the data were further analyzed using Student-Newman-Keuls *post-hoc* test for multiple comparisons. Student's *t*-test for unpaired data was used for comparison of two means. Differences were considered statistically significant if  $P < 0.05$ .

## RESULTS

In order to determine the ER-mediated effects on vascular contraction/relaxation and the downstream signaling pathways involved in the selected blood vessels, it is important to first characterize the basic contractile properties and the vascular relaxation pathways in each specific vessel. Construction of the dose-response curve for Phe in the different vascular beds is important in order to determine the concentration required to produce a measurable submaximal contraction that is needed to test the vascular relaxation effects of ER modulators. Also, measuring the relaxation response to ACh is important in order to determine the major endothelium-dependent relaxation pathways in the different vascular beds before testing the effects of ER modulators in the specific vascular bed.

In all arteries tested, Phe caused concentration-dependent contraction that reached a maximum at 10<sup>-5</sup> M (Fig. 1). When the Phe response was measured as % of maximum contraction and the EC50 calculated, Phe was less potent in abdominal than cephalic and thoracic arteries (Fig. 1, Table 1). These experiments suggested a submaximal Phe concentration of 10<sup>-6</sup> M in mesenteric and renal artery, and 3 $\times$ 10<sup>-7</sup> M in the other arteries for all subsequent vascular relaxation experiments. Also, the magnitude and/or EC50 of Phe contraction were significantly greater in endothelium-denuded than intact thoracic and abdominal aorta (Fig. 1, Table 1), suggesting endothelial release of vasodilator substances.

In endothelium-intact vessels precontracted with Phe, ACh caused significantly greater relaxation in mesenteric and renal artery than cephalic and thoracic arteries and abdominal aorta (Fig. 2). ACh relaxation was abolished in endothelium-denuded arteries (Fig. 2), supporting a role of endothelium-derived NO, PGI<sub>2</sub> and/or EDHF.<sup>41-44</sup> In the cephalic and thoracic arteries, abdominal aorta and renal artery, NOS blockade with L-NAME abolished ACh-induced relaxation, suggesting a role of NO (Fig. 2). In contrast, the mesenteric vessels showed significant ACh relaxation in the presence of L-NAME and indomethacin, and the remaining relaxation was blocked by TEA (30 mM) (Fig. 2E), supporting a role of EDHF.

To test for ER-mediated vascular activity, the effects of ER agonists on Phe contraction were measured (Fig. 3, Table 1). In cephalic, thoracic and abdominal arteries, E2 caused concentration-dependent relaxation that reached a maximum at 10<sup>-5</sup> M. Among the cephalic and thoracic arteries, E2-induced relaxation was in thoracic aorta > carotid > pulmonary artery (Fig. 3A). E2-induced relaxation was greater in abdominal than cephalic and thoracic arteries, and was in renal > mesenteric > abdominal aorta (Fig. 3A). Similar to E2, PPT (ER $\alpha$  agonist) caused relaxation of all arteries that reached a maximum at 10<sup>-5</sup> M and was most prominent in renal and mesenteric artery (Fig. 3B). In contrast, DPN (ER $\beta$  agonist) and G1 (GPR30 agonist) did not cause significant relaxation in cephalic and thoracic arteries, but caused significant relaxation in the abdominal arteries (Fig. 3C, 3D). To test the specificity of the ER agonists, treating the vessels with the appropriate concentration of the vehicle ethanol (0.1%, for E2), or DMSO (0.1%, for PPT, DPN and G1) did not cause any significant inhibition of Phe contraction, suggesting that the relaxation observed with E2, PPT, DPN and G1 was caused by the specific compound and not by the vehicle. Also, the inhibitory effects of PPT, DPN and G1 on Phe contraction in each specific vessel were prevented in tissues pretreated with the ER $\alpha$  antagonist MPP, ER $\beta$  antagonist PHTPP, and GPR30 antagonist G15, respectively, supporting the specificity of the relaxation effects of PPT, DPN and G1.

To determine the amount of vascular ER subtypes, RT-PCR analysis revealed variable expression of ER $\alpha$  mRNA among the vessels tested, but ER $\alpha$  expression was more prominent in the carotid, abdominal aorta and renal artery (Fig. 4A). In contrast, ER $\beta$  mRNA expression was significantly greater in the carotid artery than the other vessels tested (Fig. 4B). On the other hand, GPR30 mRNA expression was greater in abdominal aorta, mesenteric and renal artery compared to cephalic and thoracic arteries (Fig. 4C). Western blots of tissue homogenate from cephalic, thoracic and abdominal arteries revealed immunoreactive bands corresponding to ER $\alpha$  at 64 kDa, ER $\beta$  at 55 kDa, and GPR30 at 50 kDa (Fig. 5). Optical density analysis revealed that the amount of ER $\alpha$  was significantly greater in abdominal aorta and renal artery compared to cephalic and thoracic arteries (Fig. 5A). Also, the protein amount of ER $\beta$  was significantly greater in abdominal aorta and mesenteric artery than the carotid and pulmonary artery (Fig. 5B). Similarly, the protein amount of GPR30 was significantly greater in abdominal aorta and renal artery than the carotid and pulmonary artery (Fig. 5C).

To investigate the post-ER signaling pathways and the contribution of NO, PGI<sub>2</sub> and hyperpolarization factor to ER-mediated vascular relaxation, the effects of ER agonists were tested in vessels pretreated with the NOS inhibitor L-NAME, COX inhibitor indomethacin, and the hyperpolarization inhibitor TEA. NOS blockade by L-NAME inhibited E2-induced relaxation mainly in the thoracic aorta (Fig. 6). Similarly, PPT-induced relaxation was inhibited by L-NAME in the thoracic aorta and pulmonary artery, but not abdominal arteries (Fig. 7). The DPN (ER $\beta$  agonist)-induced small relaxation in thoracic aorta was abolished by L-NAME (Fig. 8A). In contrast, DPN caused minimal relaxation in the carotid and pulmonary artery (Fig. 8B, 8C), some relaxation in abdominal aorta (Fig. 6D), and a greater relaxation in the mesenteric and renal artery, that was not significantly affected by L-

NAME, indomethacin or TEA (Fig. 8E, 8F). Similarly, G1 (GPR30 agonist) caused minimal relaxation in the cephalic and thoracic arteries (Fig. 9A, 9B, 9C), but greater relaxation in abdominal arteries that was not significantly affected by L-NAME, indomethacin and TEA (Fig. 9D, 9E, 9F). Collectively, in the thoracic aorta, E2, PPT and DPN, but not G1 caused measurable relaxation that was inhibited by L-NAME alone, and indomethacin and TEA did not cause any further inhibition of E2, PPT or DPN-induced relaxation (Fig. 6A, 7A, 8A, 9A), suggesting ER-mediated stimulation of the NO pathway in thoracic aorta. To confirm that the ER agonists function in part by stimulating NO release, NOx was measured in thoracic aorta because it showed a significant L-NAME sensitive relaxation. In contrast, smaller vessels such as the mesenteric artery showed little L-NAME sensitive relaxation, suggesting a little role of endothelium-derived NO production, and therefore these vessels may not be suitable for testing the effects of ER agonists on NOx. Similar to ACh, E2, PPT and DPN caused significant increase in NOx production in thoracic aorta (Fig. 10). In contrast, G1 did not cause any significant increase in NOx (Fig. 10).

To investigate ER-mediated endothelium-independent inhibitory effects on VSM, experiments on endothelium-denuded arteries showed that E2, PPT, DPN and G1 caused greater relaxation in abdominal than cephalic and thoracic arteries (Fig. 11, Table 1). Membrane depolarization by high KCl is known to activate Ca<sup>2+</sup> entry through Ca<sup>2+</sup> channels into VSM.<sup>7, 39</sup> To investigate whether ER-mediated effects on arterial contraction involve inhibition of Ca<sup>2+</sup> entry into VSM, we tested the effects of ER agonists on 96 mM KCl-induced contraction in endothelium-denuded arteries. E2 caused relaxation of KCl contraction that was more prominent in the mesenteric and renal artery compared to the other vessels (Fig. 12A). Also, PPT, DPN and G1 caused significant relaxation of KCl contraction that was essentially greater in abdominal than cephalic and thoracic arteries (Fig. 12B, 12C, 12D).

## DISCUSSION

The main findings of the present study are: 1) The cephalic, thoracic and abdominal vasculature demonstrate subtype-specific ER-mediated vasodilation, 2) the regional differences in ER-mediated vasodilation are associated with differences in the expression of vascular ER subtypes, and 3) the regional differences in ER-mediated vasodilation are associated with additional differences in the post-ER endothelium-dependent pathways of vascular relaxation and endothelium-independent inhibitory effects on Ca<sup>2+</sup>-dependent mechanisms of VSM contraction.

Previous studies demonstrated significant vasodilator effects of E2.<sup>4, 6, 10, 15, 17, 19, 30</sup> Because these studies often examined the role of one ER subtype in one blood vessel, it has been difficult to relate the findings from these separate studies to each other, or to determine the contribution of the different ER subtypes to vasodilation in different blood vessels. In this study, we examined the differences in ER expression/activity in six major cephalic, thoracic and abdominal arteries with significant contractile response to the  $\alpha$ -adrenergic agonist Phe and measurable endothelium-dependent relaxation to ACh. In many vessels, ACh-induced relaxation involves activation of the NO-cGMP pathway.<sup>45, 46</sup> Consistent with these reports, in the cephalic and thoracic arteries, ACh-induced relaxation appeared to involve NO because it was inhibited by the NOS inhibitor L-NAME. Also, ACh stimulated NO production in thoracic aorta. In contrast, in mesenteric artery, a large portion of ACh relaxation appeared to involve a hyperpolarization pathway, because a significant ACh relaxation remained in the presence of L-NAME and indomethacin, and was abolished by TEA.



Using these major cephalic, thoracic and abdominal vessels, we reasoned that if vascular ER subtypes are differentially distributed in the systemic circulation, then specific ER agonists should produce distinct vasodilation responses in different vessels. E2 binds to all ERs, and its vasorelaxant effects likely involve activation of most ER subtypes.<sup>4, 15, 20</sup> On the other hand, the availability of specific ER agonists allows examination of the contribution of a specific ER subtype to the effects of E2. PPT is a selective ER $\alpha$  agonist,<sup>34, 35</sup> DPN is a selective ER $\beta$  agonist,<sup>36</sup> while G1 is a selective agonist of GPR30,<sup>37, 38</sup> a new transmembrane protein that binds E2 and mediates some of its rapid non-genomic effects.<sup>25-28</sup> In the present study, both E2 and the ER $\alpha$  agonist PPT caused almost similar relaxation profile in the cephalic, thoracic and abdominal arteries, suggesting prominent role of ER $\alpha$  in E2-induced relaxation. These findings are consistent with reports that E2 causes acute relaxation of rat aorta solely through ER $\alpha$ ,<sup>47</sup> and that both the ER $\alpha$  activator PPT<sup>34, 35</sup> and ER $\beta$  agonist DPN<sup>36</sup> cause acute relaxation in isolated rat mesenteric arteries, although PPT produces greater effect.<sup>48</sup> While DPN- and G1-induced relaxation was smaller than that of E2 and PPT, it was more prominent in the mesenteric and renal arteries than the carotid and thoracic arteries. These data are consistent with our previous report that GPR30 stimulation had little effect on contraction of the aorta of female Sprague-Dawley rat.<sup>31</sup> Other studies have shown that G1 produces vasodilation that is not different from E2 in common carotid artery of Sprague-Dawley rat of both gender,<sup>49</sup> and mesenteric artery of male Sprague-Dawley rat<sup>50</sup> and female mRen2.Lewis rat.<sup>24</sup> The present data are in agreement with a prominent vasorelaxant effect of G1 in the mesenteric artery, but demonstrate little vasorelaxant effect of G1 in the carotid and thoracic arteries. These findings highlight the importance of examining the vasorelaxation effects of G1 and other GPR30 agonists in different blood vessels from the same species, and further clarifying the role of GPR30 in the regulation of vascular function in various vascular beds.

The differences in ER-mediated vasodilation in the cephalic, thoracic and abdominal arteries could be partly due to differences in the vascular expression of ER subtypes. Earlier studies have identified ERs in mouse and rat aorta<sup>30, 51</sup> and carotid artery<sup>23, 49</sup> and rat aorta. Studies have also shown ER $\alpha$ -mediated protective effects of E2 in mouse model of carotid arterial injury,<sup>23</sup> and a prominent ER $\alpha$  signal in rat cerebral and coronary artery.<sup>52</sup> Other studies have shown predominant ER $\beta$  and small amounts of ER $\alpha$  in baboon carotid artery,<sup>53</sup> and suggested an essential role for ER $\beta$  in the regulation of vascular function and blood pressure.<sup>22</sup> GPR30 immunoreactivity was also observed in endothelial and VSM cells of Sprague-Dawley rat carotid arteries from both genders,<sup>49</sup> and in mesenteric artery endothelial and VSM cells of mRen2.Lewis female rat.<sup>24</sup> Because many of these studies were conducted on one blood vessel or focused on one ER subtype, it has been difficult to determine the relative expression of different ER subtypes in different vascular beds. The present study demonstrated an increase in both ER $\alpha$  mRNA expression and protein amount in abdominal aorta and renal artery, suggesting synchronized regulation of ER $\alpha$  at the gene transcription and protein translation level in the abdominal vasculature. Despite the increased ER $\alpha$  mRNA expression in the carotid artery, the protein amount was reduced, suggesting that the amount of ER $\alpha$  is further controlled at the protein translation/degradation level. Likewise, ER $\beta$  mRNA expression was greater while the protein amount was smaller in the carotid than the other vessels, supporting that the amount of ER $\beta$  is further regulated at the protein translation/degradation level. The tight regulation of ER $\alpha$  and ER $\beta$  mRNA expression and protein amount in the carotid artery is in accordance with the critical role of the carotid artery in controlling the blood flow to the brain centers.

Consistent with the increased DPN-induced relaxation in abdominal arteries, the protein amount of ER $\beta$  was upregulated in abdominal aorta and mesenteric artery. Also, consistent with the increased vasodilator effects of G1 in the renal artery, the GPR30 mRNA expression and protein amount were upregulated in the renal artery. Although the mesenteric

artery demonstrated increased vasodilator effects to G1 and increased GPR30 mRNA expression, it did not show an increase in GPR30 protein amount. These findings suggest that the increased vasodilator effects of ER agonists may not only be due to increased amount of the specific ERs, but could also involve increased signaling mechanisms downstream from ER activation.

E2 binds ERs and induces both genomic and nongenomic effects that promote arterial dilation.<sup>4, 14, 15, 54</sup> E2 promotes vasodilation by activating endothelium-dependent NO-cGMP, PGI<sub>2</sub>-cAMP, and EDHF relaxation pathway.<sup>4, 14</sup> E2-induced vasodilator pathways appear to be blood vessel-specific. E2 via ER $\alpha$  upregulates eNOS mRNA and protein expression and stimulates eNOS activity in bovine pulmonary artery endothelial cells,<sup>55, 56</sup> suggesting a role of ER $\alpha$  in the regulation of endothelial eNOS expression and NO production.<sup>57</sup> Other studies have shown that physiologic levels of E2 acting via ERs cause upregulation of COX-1 expression and PGI<sub>2</sub> synthesis in pulmonary artery endothelial cells.<sup>58</sup> Also, in the carotid artery of Sprague-Dawley rat G1-induced relaxation is abolished by endothelium removal or in the presence of L-NAME, suggesting a GPR30-mediated endothelium-derived NO-dependent relaxation.<sup>49</sup> To investigate the ER-mediated endothelium-dependent signaling mechanisms, the effects of ER agonists were tested in vessels treated with the NOS inhibitor L-NAME, COX inhibitor indomethacin, and hyperpolarization inhibitor TEA. In the cephalic and thoracic arteries, particularly the thoracic aorta, the vasodilator effects of E2, PPT and DPN appear to involve NO production because: 1) E2-, PPT- and DPN-induced aortic relaxation was inhibited by the NOS inhibitor L-NAME, 2) blockade of COX and PGI<sub>2</sub> production using indomethacin and the BK<sub>Ca</sub>-dependent hyperpolarization pathway using TEA did not cause further inhibition of E2-, PPT- and DPN-induced aortic relaxation, and 3) E2, PPT and DPN increased aortic NO<sub>x</sub> production. In comparison with the cephalic and thoracic arteries, E2, PPT, DPN and G1-induced relaxation in the abdominal aorta, mesenteric and renal artery was not significantly blocked by L-NAME, suggesting little role of NO in ER $\alpha$ , ER $\beta$  and GPR30-mediated relaxation in the abdominal circulation. We should note that ACh-induced relaxation in the mesenteric artery was partially inhibited by L-NAME and indomethacin, but abolished in the presence of TEA. Thus one possible explanation of the vasorelaxant effects of PPT, DPN and G1 in the abdominal arteries is that ER $\alpha$ , ER $\beta$  and GPR30 may be coupled to EDHF-mediated hyperpolarization, which in turn causes reduction in VSM [Ca<sup>2+</sup>]<sub>i</sub> and leads to vascular relaxation.<sup>59</sup> This is supported by previously reported ER $\beta$ -mediated and DPN-induced vasorelaxation effects via EDHF in murine femoral artery<sup>60</sup> and porcine coronary artery.<sup>61</sup> However, the present observation that PPT, DPN and G1-induced relaxation of abdominal arteries was not blocked by TEA suggests activation of other ER-mediated pathways of vascular relaxation that could involve TEA-insensitive small or intermediate conductance Ca<sup>2+</sup>-activated K<sup>+</sup> channels or direct effects on the mechanisms of VSM contraction.

Previous studies have shown that E2 causes vascular relaxation in endothelium-denuded aorta and coronary artery.<sup>10, 19, 62</sup> Also, E2 inhibits Phe and prostaglandin F<sub>2</sub> $\alpha$ -induced contraction in VSM cells isolated from rat aorta and porcine coronary artery.<sup>7, 63</sup> The present study demonstrated ER-mediated vasodilation in endothelium-denuded cephalic, thoracic and abdominal arteries, suggesting modulation of the VSM contraction mechanisms. Also, ER agonists inhibited high KCl-induced contraction in the cephalic, thoracic and abdominal arteries. Because KCl contraction mainly involves Ca<sup>2+</sup> entry through voltage-gated channels,<sup>7, 39</sup> the ER-mediated inhibition of KCl-induced contraction is likely due to inhibition of Ca<sup>2+</sup> entry mechanisms. This is consistent with reports that E2 decreases KCl-induced Ca<sup>2+</sup> influx in endothelium-denuded rat aorta and coronary artery strips and in isolated rat aortic VSM cells.<sup>7, 10, 64</sup> We do not wish to draw conclusions on whether E2 or subtype-specific ER agonists inhibit Ca<sup>2+</sup> entry via direct or indirect action

on plasmalemmal  $\text{Ca}^{2+}$  channels. Studies have suggested that E2 possibly via  $\text{ER}\beta$  could induce EDHF release in female mouse femoral artery,<sup>60</sup> which could cause membrane hyperpolarization and inhibition of  $\text{Ca}^{2+}$  entry through voltage-gated channels. Other studies have shown that E2 blocks  $\text{Ca}^{2+}$  channels in cultured A7r5 and aortic VSM cells.<sup>65, 66</sup> The similarity in the inhibitory effects of E2 and the  $\text{ER}\alpha$  agonist PPT on Phe contraction in endothelium-denuded arteries supports that  $\text{ER}\alpha$  is a major mediator of the effects of E2 in VSM. Importantly, the PPT, DPN and G1-induced endothelium-independent relaxation and inhibition of KCl contraction were greater in abdominal than cephalic and thoracic arteries, consistent with possible increase in the relative expression of  $\text{ER}\alpha$ ,  $\text{ER}\beta$  and GPR30 in VSM cells of abdominal arteries.

The present study demonstrated maximal vascular effects of E2 at micromolar concentrations. These concentrations are higher than the physiological plasma E2 levels in the nanomolar range. We should note that E2 is a lipophilic compound, and its plasma concentration may not reflect its vascular tissue level. Because of its lipophilic properties, prolonged exposure to nanomolar concentrations of E2 could lead to gradual tissue accumulation that eventually reaches levels equivalent to those used in the present acute studies, and these possibilities need to be examined in future studies. Also, although the observed rapid ER-mediated vascular relaxation was generally associated with parallel changes in ER expression, some exceptions were observed. For example, in the mesenteric arteries the increased GPR30-mediated vasodilation was associated with increased GPR30 mRNA expression, but decreased protein amount. Also, the  $\text{ER}\alpha$ - and  $\text{ER}\beta$ -mediated relaxation was less in the carotid artery than the abdominal arteries, although the  $\text{ER}\alpha$  and  $\text{ER}\beta$  mRNA expression was increased, while the protein amount was decreased. These discrepancies can be related to the fact that vascular ERs are involved in multiple cell functions other than rapid vasodilation including nuclear events and genomic effects. Also, it is not unlikely that some of the vascular ERs measured in the RT-PCR and Western blot analyses represent spare non-functional ER variants. Although the percent occupancy of the receptors by steroid hormones is often thought to be paralleled by the magnitude of the hormone response,<sup>67</sup> this may not always be the case. While the steroid response is generally dependent on the availability of steroid receptors, E2 dose-response studies in cell lines that stably express ERs have shown that the receptors are limiting below 500,000 ERs per cell, but at higher ER titers there are spare receptors.<sup>68</sup> Also, studies with  $17\beta$ -[6,7- $^3\text{H}$ ]E2 in specimens of human mammary tumor biopsies have shown spare receptor sites that are not saturated by the endogenous hormone. Interestingly, the average concentration of spare ERs in primary mammary tumors was higher in specimens from postmenopausal than premenopausal women<sup>69</sup>, which could partly explain the decreased vascular effects of E2 in aging women. We should also note that while the present study measured ER expression/activity in six major cephalic, thoracic and abdominal vessels, that does not minimize the importance of measuring ERs in other vessels particularly the small mesenteric resistance microvessels, and specialized vessels such as the coronary and cerebral arteries. Also, while the present study measured the total vascular tissue amount of ERs, it did not examine the relative cellular distribution of ER in the endothelium and VSM, or the subcellular distribution in these vascular cells. Previous imaging studies were able to localize  $\text{ER}\alpha$  in *en face* endothelium of female rat cerebral and coronary artery.<sup>52</sup> Also, we previously examined  $\text{ER}\alpha$ ,  $\text{ER}\beta$ , and GPR30 in single VSMCs isolated from female rat aorta using fluorescence microscopy.<sup>31</sup> Optical dissection of the subcellular distribution of  $\text{ER}\alpha$  and  $\text{ER}\beta$  revealed small amount in the cell periphery, and greater amounts in the cytosol and nucleus. In contrast, GPR30 was mainly in the cytosol, with smaller amounts in the cell periphery and nucleus.<sup>31</sup> Studying the relative distribution of ER subtypes in VSM from different vascular beds, and the changes in their distribution during ER agonist stimulation should represent an important area for future investigation.

In conclusion, ER-mediated vasodilation exhibit regional differences that are both ER agonist- and blood vessel-specific, with the cephalic and thoracic vasculature demonstrating similar relaxation to E2 and ER $\alpha$  agonist, and the abdominal vasculature demonstrating greater relaxation to ER $\beta$  and GPR30 agonists. The increased E2-mediated relaxation in abdominal arteries partly involves increased expression of ER $\beta$  and GPR30. ER-mediated relaxation likely involves endothelium-dependent NO pathway in the cephalic and thoracic arteries, but could involve a hyperpolarization pathway in the mesenteric arteries. An ER-mediated endothelium-independent inhibition of the Ca<sup>2+</sup> entry mechanisms of VSM contraction is more prominent in the abdominal than cephalic and thoracic arteries, consistent with the possibility of increased expression of ER $\alpha$ , ER $\beta$  and GPR30 in VSM cells of abdominal arteries.

## Perspective

Despite the protective vascular effects of E2 demonstrated in experimental and initial observational studies, recent clinical trials suggest that menopausal hormone therapy (MHT) may not have systemic vascular benefits, and may in effect increase the risk of vascular disease. The lack of systemic vascular benefits of MHT may be related to the type of estrogen, dose, formulation, patient's age, and age-related changes in vascular ER amount and activity, but could also be related to regional differences in the vascular ERs and post-ER signaling pathways. In systemic vascular disease there is often an assumption that findings in one representative blood vessel may be generalized to other vessels in the circulation. However, in a systemic disease such as hypertension the cellular and signaling changes observed in one blood vessel such as the aorta may be different from those observed in other vessels such as the renal and mesenteric artery. Also, vascular pathology can be confined to a specific blood vessel in the course of localized vascular disease. The present study demonstrates that vascular ERs exhibit regional differences in their expression and activity in blood vessels of the cephalic, thoracic and abdominal circulation. Regional differences in the expression/activity of ER subtypes may play a role in localized vascular disease such as carotid intimal hyperplasia, peripheral artery disease, thoracic and abdominal aortic aneurysm as well as in regional atherosclerotic vascular disease and other female prominent diseases such as migraine, Raynaud's disease and pulmonary hypertension. For localized vascular disease, specific drug targeting will be more advantageous. For instance, specific ER agonists could be useful in spastic occlusive artery disease, while specific ER antagonists may be beneficial in vascular diseases characterized by arterial wall distention and aneurysm. Subtype-specific ER agonists or antagonists coupled with specific targeting or drug delivery techniques such as drug-eluting stents and perivascular gel could be useful in modulating vascular ER activity in a specific blood vessel without affecting other vessels in the systemic circulation. An important question is how the regional distribution of ERs and their mediated responses would change with age or in estrogen deficiency states associated with surgical menopause. We have previously reported that ER-mediated relaxation pathways are reduced in the aorta of aging female rats<sup>70</sup> and that the vascular contraction mechanisms are enhanced in the aorta of ovariectomized compared with intact female rats.<sup>7, 16</sup> In this respect, studying the differences in ER distribution and activity in blood vessels of young versus old animals and in intact versus ovariectomized females could provide further information on the potential usefulness of a specific ER agonist in the treatment of age- and menopause-related vascular disease.

## Acknowledgments

R. A. Khalil was partly supported by grants from National Heart, Lung, and Blood Institute (HL-65998, HL-98724) and The Eunice Kennedy Shriver National Institute of Child Health and Human Development (HD-60702). Dr. Z. Yin was a visiting scholar from Tongji hospital, Huazhong University of Science & Technology, Wuhan, Hubei Province, P. R. China, and a recipient of a scholarship from the China Scholarship Council. Dr. Z. Yin's current

address is: Department of Obstetrics & Gynecology, The First Affiliated Hospital of Anhui Medical University, Hefei, Anhui, P. R. China. Dr. G. R. A. do Nascimento was a visiting researcher from Universidade Estadual de Ciências da Saúde de Alagoas-UNCISAL, Maceió, AL, Brazil.

## List of Abbreviations

<b>ACh</b>	acetylcholine
<b>DPN</b>	diarylpropionitrile
<b>EDHF</b>	endothelium-derived hyperpolarizing factor
<b>E2</b>	17 $\beta$ -estradiol
<b>eNOS</b>	endothelial nitric oxide synthase
<b>ER</b>	estrogen receptor
<b>L-NAME</b>	N $_{\omega}$ -Nitro-L-arginine methyl ester
<b>NO</b>	nitric oxide
<b>PGI<sub>2</sub></b>	prostacyclin
<b>Phe</b>	phenylephrine
<b>PPT</b>	4,4',4''-(4-propyl-[1H]-pyrazole-1,3,5-triyl)-tris-phenol
<b>TEA</b>	tetraethylammonium
<b>VSM</b>	vascular smooth muscle

## REFERENCES

1. Barrett-Connor E, Bush TL. Estrogen and coronary heart disease in women. *JAMA*. 1991; 265(14): 1861–1867. [PubMed: 2005736]
2. Gerhard M, Ganz P. How do we explain the clinical benefits of estrogen? From bedside to bench. *Circulation*. 1995; 92(1):5–8. [PubMed: 7788916]
3. Dubey RK, Imthurn B, Zacharia LC, Jackson EK. Hormone replacement therapy and cardiovascular disease: what went wrong and where do we go from here? *Hypertension*. 2004; 44(6):789–795. [PubMed: 15477384]
4. Orshal JM, Khalil RA. Gender, sex hormones, and vascular tone. *Am J Physiol Regul Integr Comp Physiol*. 2004; 286(2):R233–249. [PubMed: 14707008]
5. Mendelsohn ME, Karas RH. Molecular and cellular basis of cardiovascular gender differences. *Science*. 2005; 308(5728):1583–1587. [PubMed: 15947175]
6. Crews JK, Murphy JG, Khalil RA. Gender differences in Ca(2+) entry mechanisms of vasoconstriction in Wistar-Kyoto and spontaneously hypertensive rats. *Hypertension*. 1999; 34(4 Pt 2):931–936. [PubMed: 10523387]
7. Murphy JG, Khalil RA. Gender-specific reduction in contractility and [Ca(2+)](i) in vascular smooth muscle cells of female rat. *Am J Physiol Cell Physiol*. 2000; 278(4):C834–844. [PubMed: 10751331]
8. Li Z, Krause DN, Doolen S, Duckles SP. Ovariectomy eliminates sex differences in rat tail artery response to adrenergic nerve stimulation. *Am J Physiol*. 1997; 272(4 Pt 2):H1819–1825. [PubMed: 9139968]
9. Geary GG, Krause DN, Duckles SP. Estrogen reduces myogenic tone through a nitric oxide-dependent mechanism in rat cerebral arteries. *Am J Physiol*. 1998; 275(1 Pt 2):H292–300. [PubMed: 9688926]
10. Crews JK, Khalil RA. Antagonistic effects of 17 beta-estradiol, progesterone, and testosterone on Ca<sub>2+</sub> entry mechanisms of coronary vasoconstriction. *Arterioscler Thromb Vasc Biol*. 1999; 19(4):1034–1040. [PubMed: 10195933]

11. Mendoza SG, Zerpa A, Carrasco H, Colmenares O, Rangel A, Gartside PS, Kashyap ML. Estradiol, testosterone, apolipoproteins, lipoprotein cholesterol, and lipolytic enzymes in men with premature myocardial infarction and angiographically assessed coronary occlusion. *Artery*. 1983; 12(1):1–23. [PubMed: 6431945]
12. Bing RJ, Conforto A. Reversal of acetylcholine effect on atherosclerotic coronary arteries by estrogen: pharmacologic phenomenon of clinical importance? *J Am Coll Cardiol*. 1992; 20(2): 458–459. [PubMed: 1634686]
13. Wolinsky H. Effects of estrogen and progestogen treatment on the response of the aorta of male rats to hypertension. Morphological and chemical studies. *Circ Res*. 1972; 30(3):341–349. [PubMed: 5060434]
14. Serock MR, Wells AK, Khalil RA. Modulators of vascular sex hormone receptors and their effects in estrogen-deficiency states associated with menopause. *Recent Pat Cardiovasc Drug Discov*. 2008; 3(3):165–186. [PubMed: 18991792]
15. Mendelsohn ME. Genomic and nongenomic effects of estrogen in the vasculature. *Am J Cardiol*. 2002; 90(1A):3F–6F.
16. Kanashiro CA, Khalil RA. Gender-related distinctions in protein kinase C activity in rat vascular smooth muscle. *Am J Physiol Cell Physiol*. 2001; 280(1):C34–45. [PubMed: 11121374]
17. Gisclard V, Miller VM, Vanhoutte PM. Effect of 17 beta-estradiol on endothelium-dependent responses in the rabbit. *J Pharmacol Exp Ther*. 1988; 244(1):19–22. [PubMed: 3121846]
18. Herrington DM, Braden GA, Williams JK, Morgan TM. Endothelial-dependent coronary vasomotor responsiveness in postmenopausal women with and without estrogen replacement therapy. *Am J Cardiol*. 1994; 73(13):951–952. [PubMed: 8184850]
19. Jiang CW, Sarrel PM, Lindsay DC, Poole-Wilson PA, Collins P. Endothelium-independent relaxation of rabbit coronary artery by 17 beta-oestradiol in vitro. *Br J Pharmacol*. 1991; 104(4): 1033–1037. [PubMed: 1810590]
20. Smiley DA, Khalil RA. Estrogenic compounds, estrogen receptors and vascular cell signaling in the aging blood vessels. *Curr Med Chem*. 2009; 16(15):1863–1887. [PubMed: 19442151]
21. Chambliss KL, Yuhanna IS, Mineo C, Liu P, German Z, Sherman TS, Mendelsohn ME, Anderson RG, Shaul PW. Estrogen receptor alpha and endothelial nitric oxide synthase are organized into a functional signaling module in caveolae. *Circ Res*. 2000; 87(11):E44–52. [PubMed: 11090554]
22. Zhu Y, Bian Z, Lu P, Karas RH, Bao L, Cox D, Hodgin J, Shaul PW, Thoren P, Smithies O, Gustafsson JA, Mendelsohn ME. Abnormal vascular function and hypertension in mice deficient in estrogen receptor beta. *Science*. 2002; 295(5554):505–508. [PubMed: 11799247]
23. Pare G, Krust A, Karas RH, Dupont S, Aronovitz M, Chambon P, Mendelsohn ME. Estrogen receptor-alpha mediates the protective effects of estrogen against vascular injury. *Circ Res*. 2002; 90(10):1087–1092. [PubMed: 12039798]
24. Lindsey SH, Carver KA, Prossnitz ER, Chappell MC. Vasodilation in response to the GPR30 agonist G-1 is not different from estradiol in the mRen2.Lewis female rat. *J Cardiovasc Pharmacol*. 2011; 57(5):598–603. [PubMed: 21326105]
25. Revankar CM, Cimino DF, Sklar LA, Arterburn JB, Prossnitz ER. A transmembrane intracellular estrogen receptor mediates rapid cell signaling. *Science*. 2005; 307(5715):1625–1630. [PubMed: 15705806]
26. Filardo E, Quinn J, Pang Y, Graeber C, Shaw S, Dong J, Thomas P. Activation of the novel estrogen receptor G protein-coupled receptor 30 (GPR30) at the plasma membrane. *Endocrinology*. 2007; 148(7):3236–3245. [PubMed: 17379646]
27. Haas E, Meyer MR, Schurr U, Bhattacharya I, Minotti R, Nguyen HH, Heigl A, Lachat M, Genoni M, Barton M. Differential effects of 17beta-estradiol on function and expression of estrogen receptor alpha, estrogen receptor beta, and GPR30 in arteries and veins of patients with atherosclerosis. *Hypertension*. 2007; 49(6):1358–1363. [PubMed: 17452498]
28. Prossnitz ER, Oprea TI, Sklar LA, Arterburn JB. The ins and outs of GPR30: a transmembrane estrogen receptor. *J Steroid Biochem Mol Biol*. 2008; 109(3-5):350–353. [PubMed: 18406603]
29. Raffetto JD, Qiao X, Beauregard KG, Khalil RA. Estrogen receptor-mediated enhancement of venous relaxation in female rat: implications in sex-related differences in varicose veins. *J Vasc Surg*. 2010; 51(4):972–981. [PubMed: 20347696]

30. Rubanyi GM, Freay AD, Kauser K, Sukovich D, Burton G, Lubahn DB, Couse JF, Curtis SW, Korach KS. Vascular estrogen receptors and endothelium-derived nitric oxide production in the mouse aorta. Gender difference and effect of estrogen receptor gene disruption. *J Clin Invest*. 1997; 99(10):2429–2437. [PubMed: 9153286]
31. Ma Y, Qiao X, Falone AE, Reslan OM, Sheppard SJ, Khalil RA. Gender-specific reduction in contraction is associated with increased estrogen receptor expression in single vascular smooth muscle cells of female rat. *Cell Physiol Biochem*. 2010; 26(3):457–470. [PubMed: 20798531]
32. Mazzuca MQ, Wlodek ME, Dragomir NM, Parkington HC, Tare M. Uteroplacental insufficiency programs regional vascular dysfunction and alters arterial stiffness in female offspring. *J Physiol*. 2010; 588(Pt 11):1997–2010. [PubMed: 20403978]
33. Yener T, Turkkani Tunc A, Aslan H, Aytan H, Cantug Caliskan A. Determination of oestrous cycle of the rats by direct examination: how reliable? *Anat Histol Embryol*. 2007; 36(1):75–77. [PubMed: 17266672]
34. Sun J, Meyers MJ, Fink BE, Rajendran R, Katzenellenbogen JA, Katzenellenbogen BS. Novel ligands that function as selective estrogens or antiestrogens for estrogen receptor-alpha or estrogen receptor-beta. *Endocrinology*. 1999; 140(2):800–804. [PubMed: 9927308]
35. Stauffer SR, Coletta CJ, Tedesco R, Nishiguchi G, Carlson K, Sun J, Katzenellenbogen BS, Katzenellenbogen JA. Pyrazole ligands: structure-affinity/activity relationships and estrogen receptor-alpha-selective agonists. *J Med Chem*. 2000; 43(26):4934–4947. [PubMed: 11150164]
36. Harrington WR, Sheng S, Barnett DH, Petz LN, Katzenellenbogen JA, Katzenellenbogen BS. Activities of estrogen receptor alpha- and beta-selective ligands at diverse estrogen responsive gene sites mediating transactivation or transrepression. *Mol Cell Endocrinol*. 2003; 206(1-2):13–22. [PubMed: 12943986]
37. Filardo EJ, Quinn JA, Bland KI, Frackelton AR Jr. Estrogen-induced activation of Erk-1 and Erk-2 requires the G protein-coupled receptor homolog, GPR30, and occurs via trans-activation of the epidermal growth factor receptor through release of HB-EGF. *Mol Endocrinol*. 2000; 14(10):1649–1660. [PubMed: 11043579]
38. Kleuser B, Malek D, Gust R, Pertz HH, Potteck H. 17-Beta-estradiol inhibits transforming growth factor-beta signaling and function in breast cancer cells via activation of extracellular signal-regulated kinase through the G protein-coupled receptor 30. *Mol Pharmacol*. 2008; 74(6):1533–1543. [PubMed: 18768737]
39. Khalil RA, van Breemen C. Sustained contraction of vascular smooth muscle: calcium influx or C-kinase activation? *J Pharmacol Exp Ther*. 1988; 244(2):537–542. [PubMed: 3346836]
40. Giardina JB, Green GM, Rinewalt AN, Granger JP, Khalil RA. Role of endothelin B receptors in enhancing endothelium-dependent nitric oxide-mediated vascular relaxation during high salt diet. *Hypertension*. 2001; 37(2 Part 2):516–523. [PubMed: 11230328]
41. Fleming I, Busse R. NO: the primary EDRF. *J Mol Cell Cardiol*. 1999; 31(1):5–14. [PubMed: 10072711]
42. Busse R, Edwards G, Feletou M, Fleming I, Vanhoutte PM, Weston AH. EDHF: bringing the concepts together. *Trends Pharmacol Sci*. 2002; 23(8):374–380. [PubMed: 12377579]
43. Feletou M, Vanhoutte PM. Endothelium-derived hyperpolarizing factor. *Clin Exp Pharmacol Physiol*. 1996; 23(12):1082–1090. [PubMed: 8977164]
44. Parkington HC, Coleman HA, Tare M. Prostacyclin and endothelium-dependent hyperpolarization. *Pharmacol Res*. 2004; 49(6):509–514. [PubMed: 15026028]
45. Davis JR, Giardina JB, Green GM, Alexander BT, Granger JP, Khalil RA. Reduced endothelial NO-cGMP vascular relaxation pathway during TNF-alpha-induced hypertension in pregnant rats. *Am J Physiol Regul Integr Comp Physiol*. 2002; 282(2):R390–399. [PubMed: 11792648]
46. Payne JA, Alexander BT, Khalil RA. Decreased endothelium-dependent NO-cGMP vascular relaxation and hypertension in growth-restricted rats on a high-salt diet. *Hypertension*. 2004; 43(2):420–427. [PubMed: 14707161]
47. Bolego C, Cignarella A, Sanvito P, Pelosi V, Pellegatta F, Puglisi L, Pinna C. The acute estrogenic dilation of rat aorta is mediated solely by selective estrogen receptor-alpha agonists and is abolished by estrogen deprivation. *J Pharmacol Exp Ther*. 2005; 313(3):1203–1208. [PubMed: 15722404]

48. Montgomery S, Shaw L, Pantelides N, Taggart M, Austin C. Acute effects of oestrogen receptor subtype-specific agonists on vascular contractility. *Br J Pharmacol.* 2003; 139(7):1249–1253. [PubMed: 12890703]
49. Broughton BR, Miller AA, Sobey CG. Endothelium-dependent relaxation by G protein-coupled receptor 30 agonists in rat carotid arteries. *Am J Physiol Heart Circ Physiol.* 2010; 298(3):H1055–1061. [PubMed: 20061543]
50. Haas E, Bhattacharya I, Brailoiu E, Damjanovic M, Brailoiu GC, Gao X, Mueller-Guerre L, Marjon NA, Gut A, Minotti R, Meyer MR, Amann K, Ammann E, Perez-Dominguez A, Genoni M, Clegg DJ, Dun NJ, Resta TC, Prossnitz ER, Barton M. Regulatory role of G protein-coupled estrogen receptor for vascular function and obesity. *Circ Res.* 2009; 104(3):288–291. [PubMed: 19179659]
51. Lin AL, Shain SA. Estrogen-mediated cytoplasmic and nuclear distribution of rat cardiovascular estrogen receptors. *Arteriosclerosis.* 1985; 5(6):668–677. [PubMed: 4074199]
52. Dan P, Cheung JC, Scriven DR, Moore ED. Epitope-dependent localization of estrogen receptor-alpha, but not-beta, in en face arterial endothelium. *Am J Physiol Heart Circ Physiol.* 2003; 284(4):H1295–1306. [PubMed: 12531733]
53. Aavik E, du Toit D, Myburgh E, Frosen J, Hayry P. Estrogen receptor beta dominates in baboon carotid after endothelial denudation injury. *Mol Cell Endocrinol.* 2001; 182(1):91–98. [PubMed: 11500242]
54. Paredes-Carbajal MC, Juarez-Oropeza MA, Ortiz-Mendoza CM, Mascher D. Effects of acute and chronic estrogenic treatment on vasomotor responses of aortic rings from ovariectomized rats. *Life Sci.* 1995; 57(5):473–486. [PubMed: 7623614]
55. MacRitchie AN, Jun SS, Chen Z, German Z, Yuhanna IS, Sherman TS, Shaul PW. Estrogen upregulates endothelial nitric oxide synthase gene expression in fetal pulmonary artery endothelium. *Circ Res.* 1997; 81(3):355–362. [PubMed: 9285637]
56. Lantin-Hermoso RL, Rosenfeld CR, Yuhanna IS, German Z, Chen Z, Shaul PW. Estrogen acutely stimulates nitric oxide synthase activity in fetal pulmonary artery endothelium. *Am J Physiol.* 1997; 273(1 Pt 1):L119–126. [PubMed: 9252548]
57. Sumi D, Ignarro LJ. Estrogen-related receptor alpha 1 up-regulates endothelial nitric oxide synthase expression. *Proc Natl Acad Sci U S A.* 2003; 100(24):14451–14456. [PubMed: 14610283]
58. Jun SS, Chen Z, Pace MC, Shaul PW. Estrogen upregulates cyclooxygenase-1 gene expression in ovine fetal pulmonary artery endothelium. *J Clin Invest.* 1998; 102(1):176–183. [PubMed: 9649571]
59. Feletou M, Vanhoutte PM. Endothelium-derived hyperpolarizing factor: where are we now? *Arterioscler Thromb Vasc Biol.* 2006; 26(6):1215–1225. [PubMed: 16543495]
60. Luksha L, Poston L, Gustafsson JA, Hultenby K, Kublickiene K. The oestrogen receptor beta contributes to sex related differences in endothelial function of murine small arteries via EDHF. *J Physiol.* 2006; 577(Pt 3):945–955. [PubMed: 17038424]
61. Traupe T, Stettler CD, Li H, Haas E, Bhattacharya I, Minotti R, Barton M. Distinct roles of estrogen receptors alpha and beta mediating acute vasodilation of epicardial coronary arteries. *Hypertension.* 2007; 49(6):1364–1370. [PubMed: 17470727]
62. Crews JK, Khalil RA. Gender-specific inhibition of Ca<sup>2+</sup> entry mechanisms of arterial vasoconstriction by sex hormones. *Clin Exp Pharmacol Physiol.* 1999; 26(9):707–715. [PubMed: 10499160]
63. Murphy JG, Khalil RA. Decreased [Ca<sup>2+</sup>]<sub>i</sub> during inhibition of coronary smooth muscle contraction by 17beta-estradiol, progesterone, and testosterone. *J Pharmacol Exp Ther.* 1999; 291(1):44–52. [PubMed: 10490885]
64. Freay AD, Curtis SW, Korach KS, Rubanyi GM. Mechanism of vascular smooth muscle relaxation by estrogen in depolarized rat and mouse aorta. Role of nuclear estrogen receptor and Ca<sup>2+</sup> uptake. *Circ Res.* 1997; 81(2):242–248. [PubMed: 9242185]
65. Zhang F, Ram JL, Standley PR, Sowers JR. 17beta-Estradiol attenuates voltage-dependent Ca<sup>2+</sup> currents in A7r5 vascular smooth muscle cell line. *Am J Physiol.* 1994; 266(4 Pt 1):C975–980. [PubMed: 8178970]



66. Nakajima T, Kitazawa T, Hamada E, Hazama H, Omata M, Kurachi Y. 17beta-Estradiol inhibits the voltage-dependent L-type Ca<sup>2+</sup> currents in aortic smooth muscle cells. *Eur J Pharmacol.* 1995; 294(2-3):625–635. [PubMed: 8750727]
67. Baxter JD, Funder JW. Hormone receptors. *N Engl J Med.* 1979; 301(21):1149–1161. [PubMed: 226885]
68. Webb P, Lopez GN, Greene GL, Baxter JD, Kushner PJ. The limits of the cellular capacity to mediate an estrogen response. *Mol Endocrinol.* 1992; 6(2):157–167. [PubMed: 1569962]
69. Trams G, Maass H. Specific binding of estradiol and dihydrotestosterone in human mammary cancers. *Cancer Res.* 1977; 37(1):258–261. [PubMed: 830412]
70. Wynne FL, Payne JA, Cain AE, Reckelhoff JF, Khalil RA. Age-related reduction in estrogen receptor-mediated mechanisms of vascular relaxation in female spontaneously hypertensive rats. *Hypertension.* 2004; 43(2):405–412. [PubMed: 14699001]

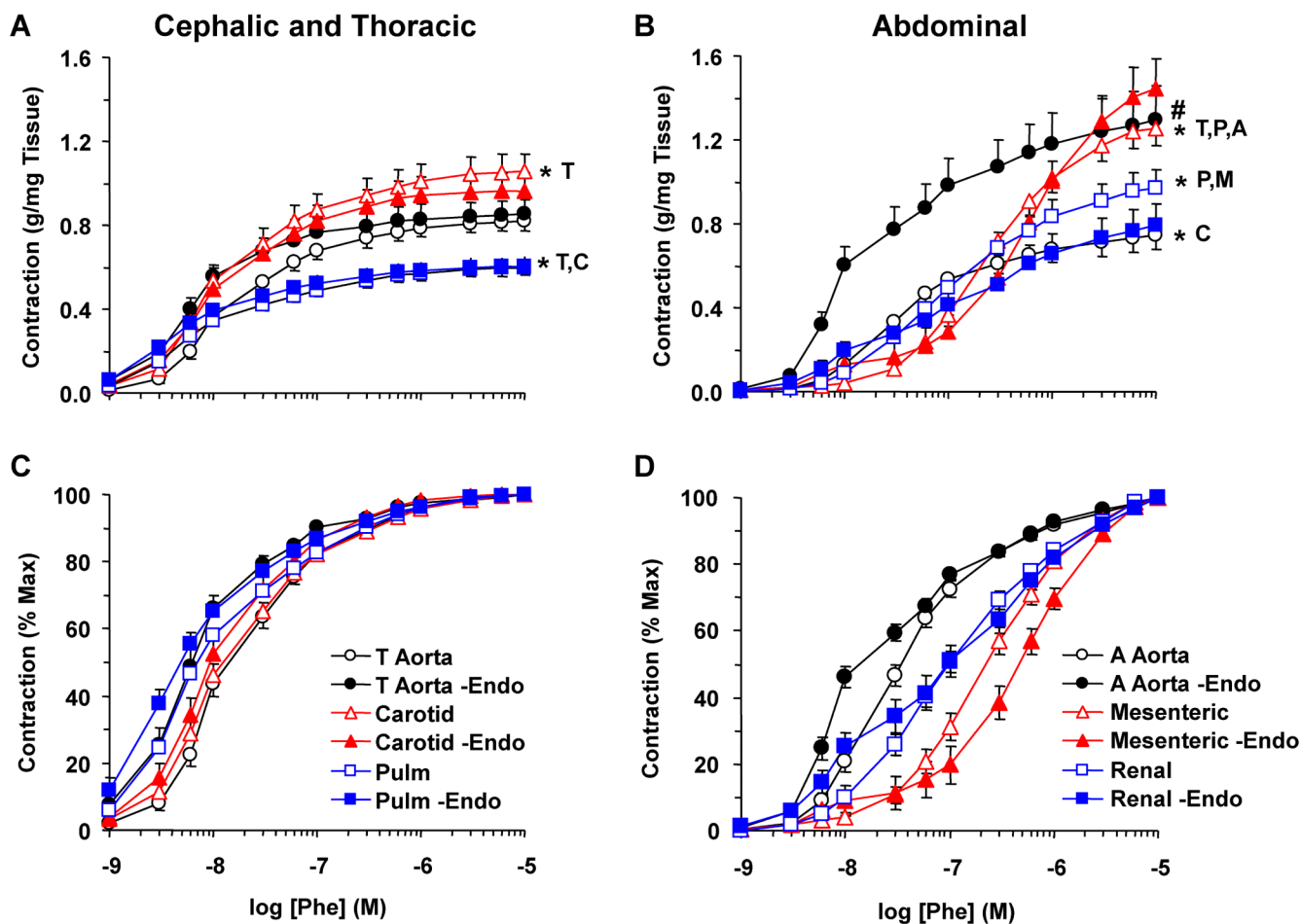


**Fig. 1.** Phe-induced contraction in cephalic, thoracic and abdominal arteries of female rat. Endothelium-intact and -denuded segments of thoracic aorta, carotid and pulmonary artery (A) as well as abdominal aorta, mesenteric and renal artery (B) were incubated in normal Krebs solution. The vessels were stimulated with the  $\alpha$ -adrenergic agonist Phe ( $10^{-9}$  to  $10^{-5}$  M) and the contractile response was recorded and presented in g/mg tissue (*Upper Panels*) or as % of maximal contraction (*Lower Panels*). The Phe response in intact vessels (+Endo) was compared with the response in endothelium-denuded vessels (-Endo). Data represent means $\pm$ SEM, n=8 to 10. \* Significantly different maximal contraction ( $p < 0.05$ ).

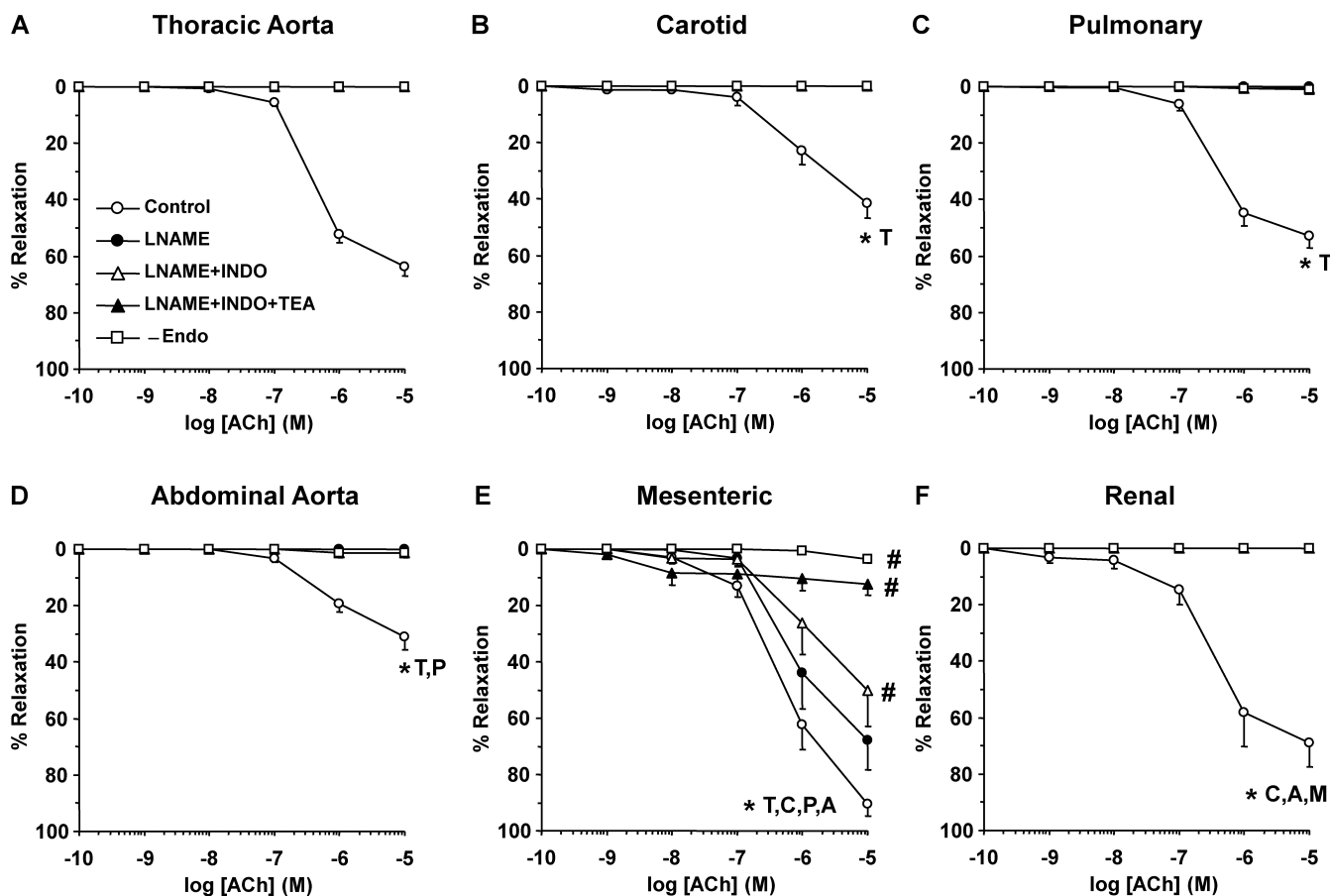


**Fig. 2.**

Acetylcholine (ACh)-induced relaxation in cephalic, thoracic and abdominal vessels of female rat. Endothelium-intact and -denuded segments of thoracic aorta (A), carotid (B) and pulmonary artery (C) as well as abdominal aorta (D), mesenteric (E) and renal artery (F) were precontracted with submaximal concentration of Phe ( $10^{-6}$  M in mesenteric and renal artery,  $3 \times 10^{-7}$  M in the other arteries) and the steady-state contraction was recorded. ACh ( $10^{-9}$  to  $10^{-5}$  M) was added and the % relaxation of Phe contraction was compared in blood vessels non-treated or treated with the NOS inhibitor L-NAME ( $3 \times 10^{-4}$  M), COX inhibitor indomethacin (INDO,  $10^{-5}$  M), and  $BK_{Ca}$  blocker TEA (30 mM). ACh-induced relaxation was also compared in intact versus endothelium-denuded arteries (-Endo). Data represent means  $\pm$  SEM, n=8 to 10. \* Significantly different maximal relaxation ( $p < 0.05$ ).

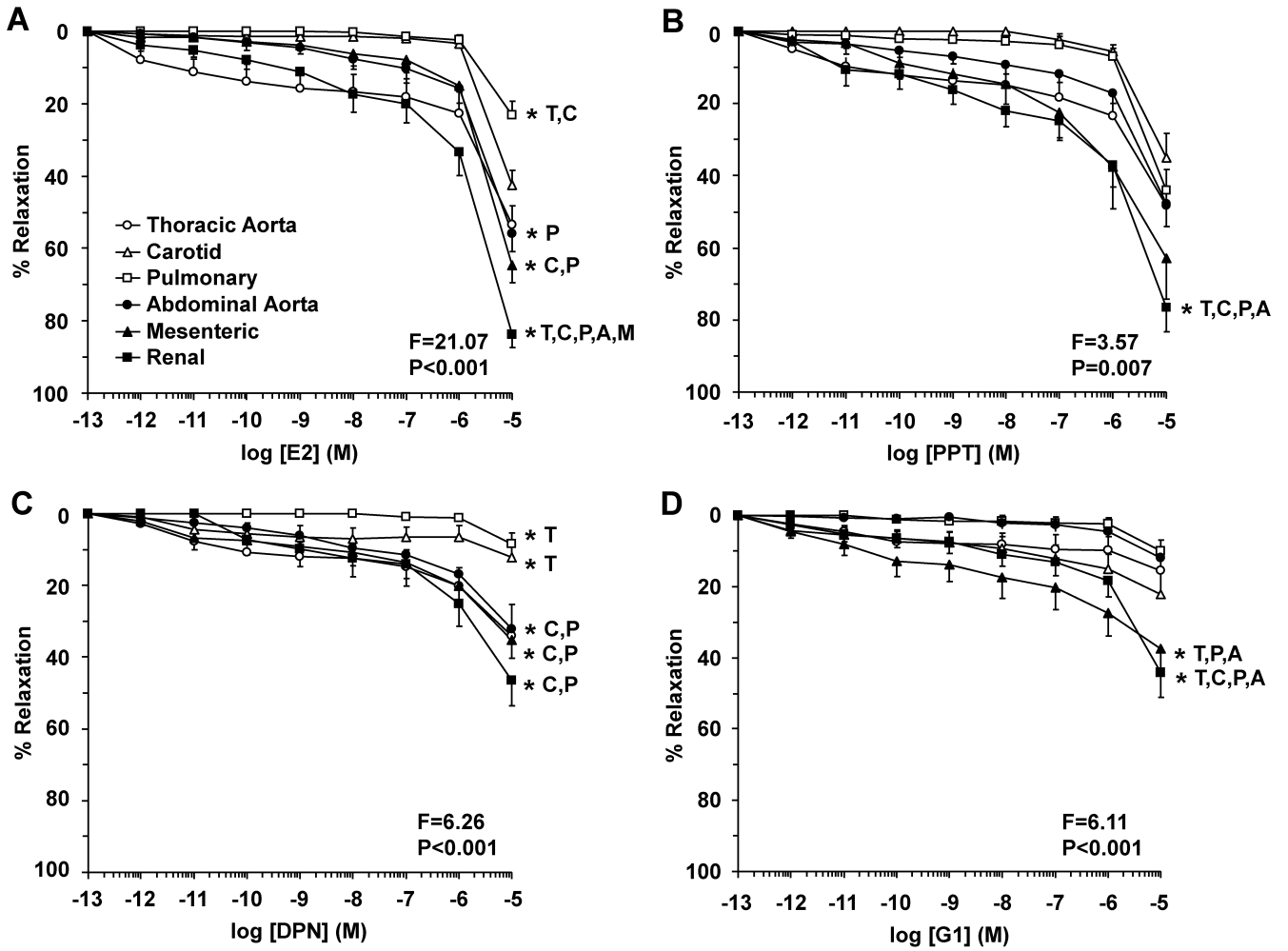


**Fig. 3.** ER-mediated relaxation in cephalic, thoracic and abdominal arteries of female rat. Endothelium-intact segments of thoracic aorta (open circles), carotid (open triangles) and pulmonary artery (open squares) as well as abdominal aorta (closed circles), mesenteric (closed triangles) and renal artery (closed squares) were precontracted with submaximal concentration of Phe and the steady-state contraction was recorded. Increasing concentrations ( $10^{-12}$  to  $10^{-5}$  M) of 17β-estradiol (E2, activator of most ERs) (A), PPT (ERα agonist) (B), DPN (ERβ agonist) (C), or G1 (GPR30 agonist) (D) were added and the % relaxation of Phe contraction was measured. Data represent means±SEM, n= 8 to 10. \* Significantly different (p<0.05) from corresponding measurement in thoracic aorta [T], carotid [C], pulmonary [P], abdominal aorta [A], mesenteric [M] and renal artery [R].

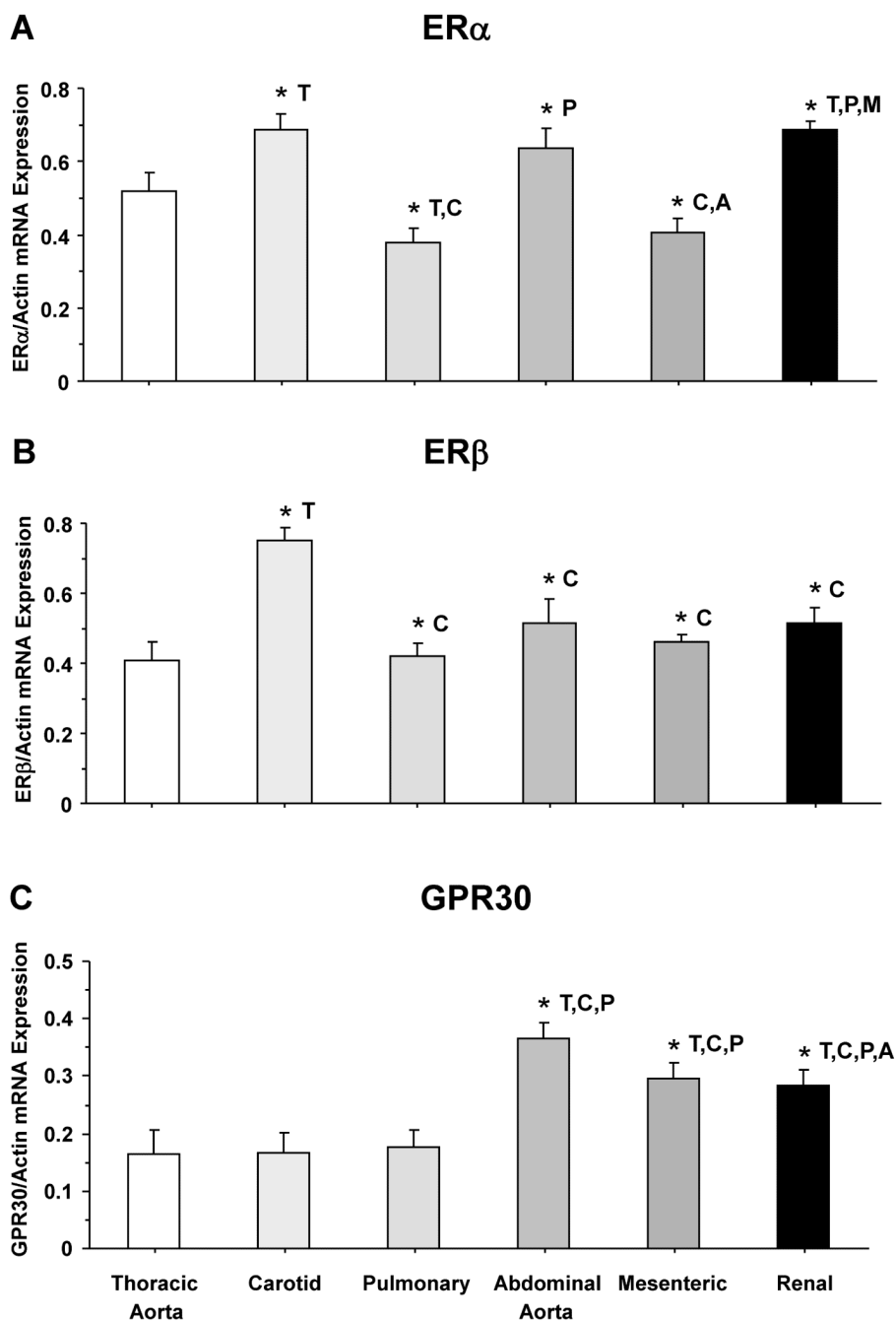


**Fig. 4.** ER $\alpha$ , ER $\beta$  and GPR30 mRNA expression in cephalic, thoracic and abdominal arteries of female rat. Tissue homogenate of thoracic aorta, carotid, pulmonary, abdominal aorta, mesenteric and renal artery were prepared for real time RT-PCR. The mRNA expression of ER $\alpha$  (A), ER $\beta$  (B), and GPR30 (C) was measured and normalized to the house-keeping gene actin. Data represent means $\pm$ SEM, n=8 to 10. \* Significantly different ( $p < 0.05$ ) from corresponding measurement in thoracic aorta [T], carotid [C], pulmonary [P], abdominal aorta [A], mesenteric [M] and renal artery [R].

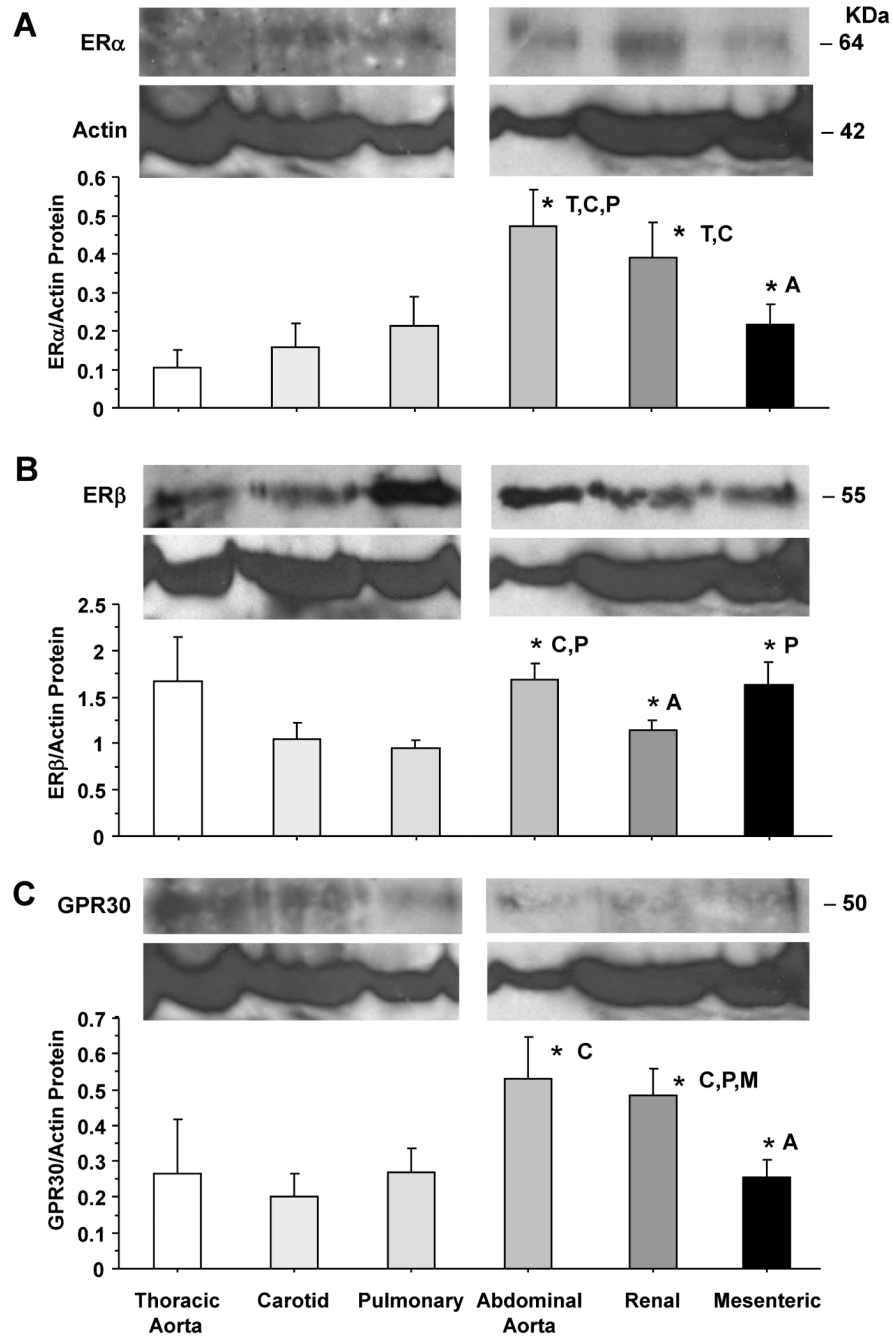


**Fig. 5.** ER $\alpha$ , ER $\beta$  and GPR30 protein amount in cephalic, thoracic and abdominal arteries of female rat. Tissue homogenate of thoracic aorta, carotid, pulmonary, abdominal aorta, renal and mesenteric artery were prepared for Western blot analysis. ER subtypes were detected using antibodies to ER $\alpha$  (1:500) (A), ER $\beta$  (1:1000) (B) and GPR30 (1:500) (C). Blots for cephalic and thoracic arteries (aorta, carotid, pulmonary) as compared to abdominal arteries (abdominal aorta, renal, mesenteric) were performed on different gels. The representative immunoblots for the abdominal aorta, renal, and mesenteric artery in panels B and C have the same actin because the blots were first reacted with GPR30 antibody, stripped, then reacted with ER $\beta$  antibody, stripped, then reacted with actin antibody. The intensity of the

immunoreactive bands was analyzed using optical densitometry, and normalized to the house keeping protein actin. Data represent means $\pm$ SEM, n= 8 to 10. \* Significantly different ( $p<0.05$ ) from corresponding measurement in thoracic aorta [T], carotid [C], pulmonary [P], abdominal aorta [A], mesenteric [M] and renal artery [R].

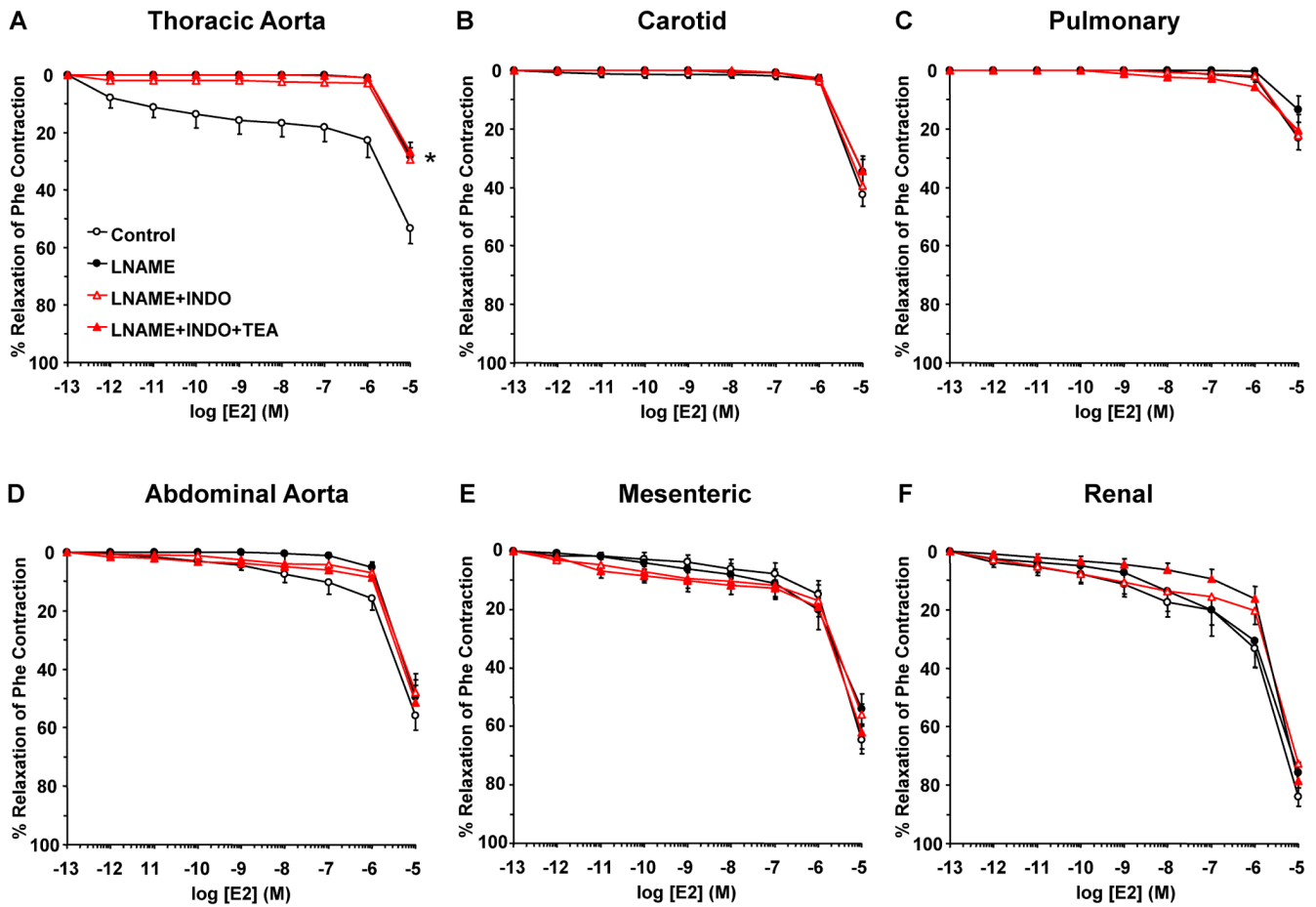


**Fig. 6.**

Contribution of NO, PGI<sub>2</sub>, and hyperpolarization factor to E2-induced relaxation of cephalic, thoracic and abdominal arteries of female rat. Endothelium-intact segments of thoracic aorta (A), carotid (B) pulmonary (C) abdominal aorta (D), mesenteric (E) and renal artery (F) were either nontreated or pretreated for 15 min with L-NAME ( $3 \times 10^{-4}$  M), L-NAME+indomethacin (INDO,  $10^{-5}$  M), or L-NAME+INDO+TEA (30 mM). The vessels were precontracted with a submaximal concentration of Phe then increasing concentrations ( $10^{-12}$  to  $10^{-5}$  M) of  $17\beta$ -estradiol (E2, activator of most ERs) were added and the % relaxation of Phe contraction was measured. Data represent means  $\pm$  SEM, n= 8 to 10. \* Significantly different ( $p < 0.05$ ) from corresponding measurements in control nontreated vessel.



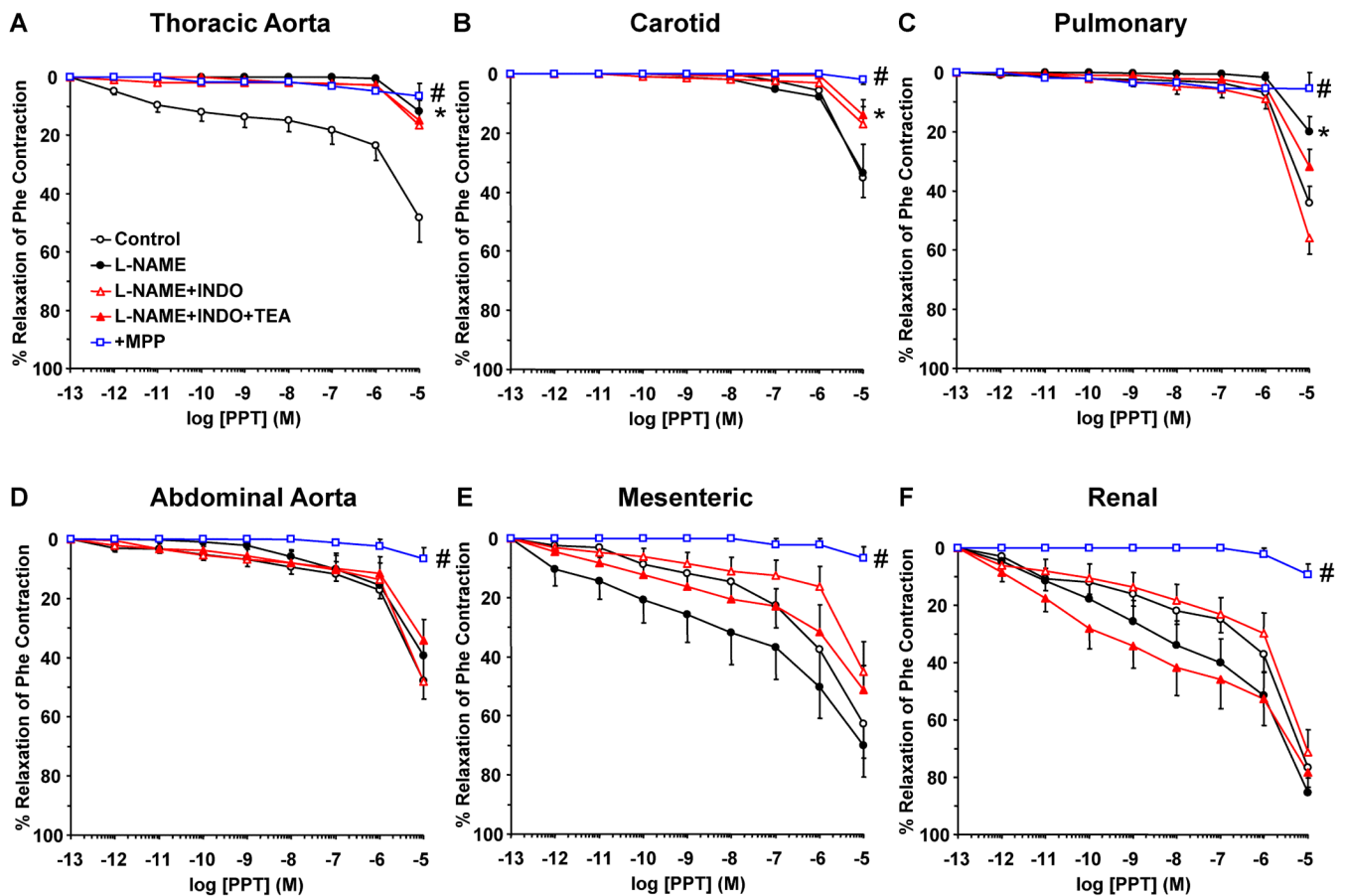


**Fig. 7.**

Contribution of NO, PGI<sub>2</sub>, and hyperpolarization factor to ER $\alpha$ -mediated relaxation of cephalic, thoracic and abdominal arteries of female rat. Endothelium-intact segments of thoracic aorta (A), carotid (B), pulmonary (C), abdominal aorta (D), mesenteric (E) and renal artery (F) were either nontreated or pretreated for 15 min with L-NAME ( $3 \times 10^{-4}$  M), L-NAME+indomethacin (INDO,  $10^{-5}$  M), or L-NAME+INDO+TEA (30 mM). The vessels were precontracted with submaximal concentration of Phe then increasing concentrations ( $10^{-12}$  to  $10^{-5}$  M) of PPT (ER $\alpha$  agonist) were added and the % relaxation of Phe contraction was measured. The specificity of the relaxation effects of PPT were tested in blood vessels pretreated with the ER $\alpha$  antagonist MPP ( $10^{-5}$  M). Data represent means  $\pm$  SEM, n = 8 to 10. \* Significantly different (p < 0.05) from corresponding measurements in control nontreated vessels. # Measurements in vessels treated with the ER $\alpha$  antagonist MPP are significantly different (p < 0.05) from corresponding measurements in control nontreated vessels.

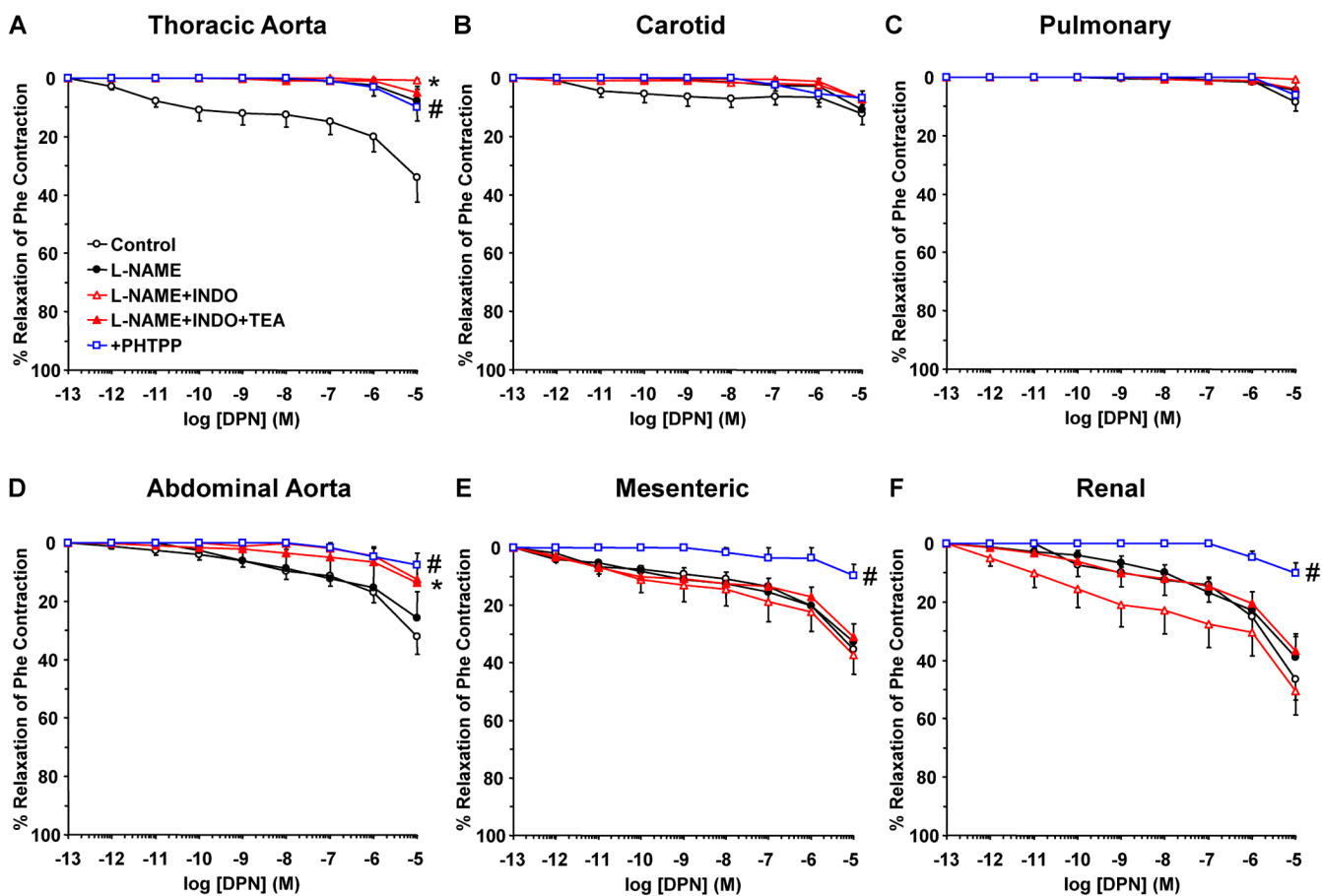


**Fig. 8.** Contribution of NO, PGI<sub>2</sub>, and hyperpolarization factor to ERβ-mediated relaxation of cephalic, thoracic and abdominal arteries of female rat. Endothelium-intact segments of thoracic aorta (A), carotid (B) pulmonary (C) abdominal aorta (D), mesenteric (E) and renal artery (F) were either nontreated or pretreated for 15 min with L-NAME ( $3 \times 10^{-4}$  M), L-NAME+indomethacin (INDO,  $10^{-5}$  M), or L-NAME+INDO+TEA (30 mM). The vessels were precontracted with submaximal concentration of Phe then increasing concentrations ( $10^{-12}$  to  $10^{-5}$  M) of DPN (ERβ agonist) were added and the % relaxation of Phe contraction was measured. The specificity of the relaxation effects of DPN were tested in blood vessels pretreated with the ERβ antagonist PHTPP ( $10^{-5}$  M). Data represent means  $\pm$  SEM, n= 8 to 10. \* Maximal relaxation is significantly different ( $p < 0.05$ ) from corresponding measurements in control nontreated vessels. # Measurements in vessels treated with the ERβ antagonist PHTPP are significantly different ( $p < 0.05$ ) from corresponding measurements in control nontreated vessels.

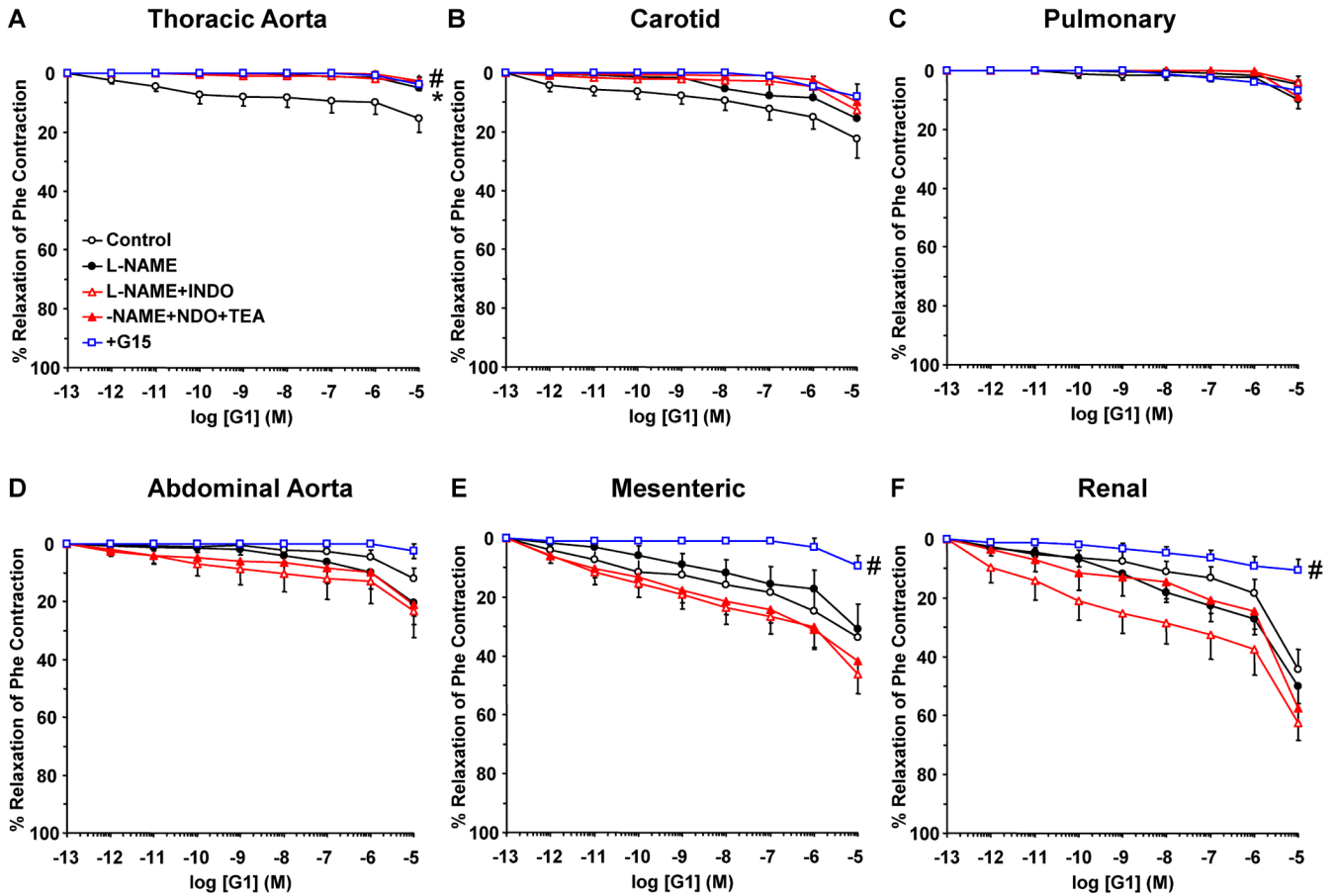


**Fig. 9.** Contribution of NO, PGI<sub>2</sub>, and hyperpolarization factor to GPR30-mediated relaxation of cephalic, thoracic and abdominal arteries of female rat. Endothelium-intact segments of thoracic aorta (A), carotid (B), pulmonary artery (C), abdominal aorta (D), mesenteric (E) and renal artery (F) were either nontreated or pretreated for 15 min with L-NAME ( $3 \times 10^{-4}$  M), L-NAME+indomethacin (INDO,  $10^{-5}$  M), or L-NAME+INDO+TEA (30 mM). The vessels were precontracted with submaximal concentration of Phe then increasing concentrations ( $10^{-12}$  to  $10^{-5}$  M) of G1 (GPR30 agonist) were added and the % relaxation of Phe contraction was measured. The specificity of the relaxation effects of G1 were tested in blood vessels pretreated with the GPR30 antagonist G15 ( $10^{-5}$  M). Data represent means  $\pm$  SEM, n= 8 to 10. \* Maximal relaxation is significantly different ( $p < 0.05$ ) from corresponding measurements in control nontreated vessels. # Measurements in vessels treated with the GPR30 antagonist G15 are significantly different ( $p < 0.05$ ) from corresponding measurements in control nontreated vessels.

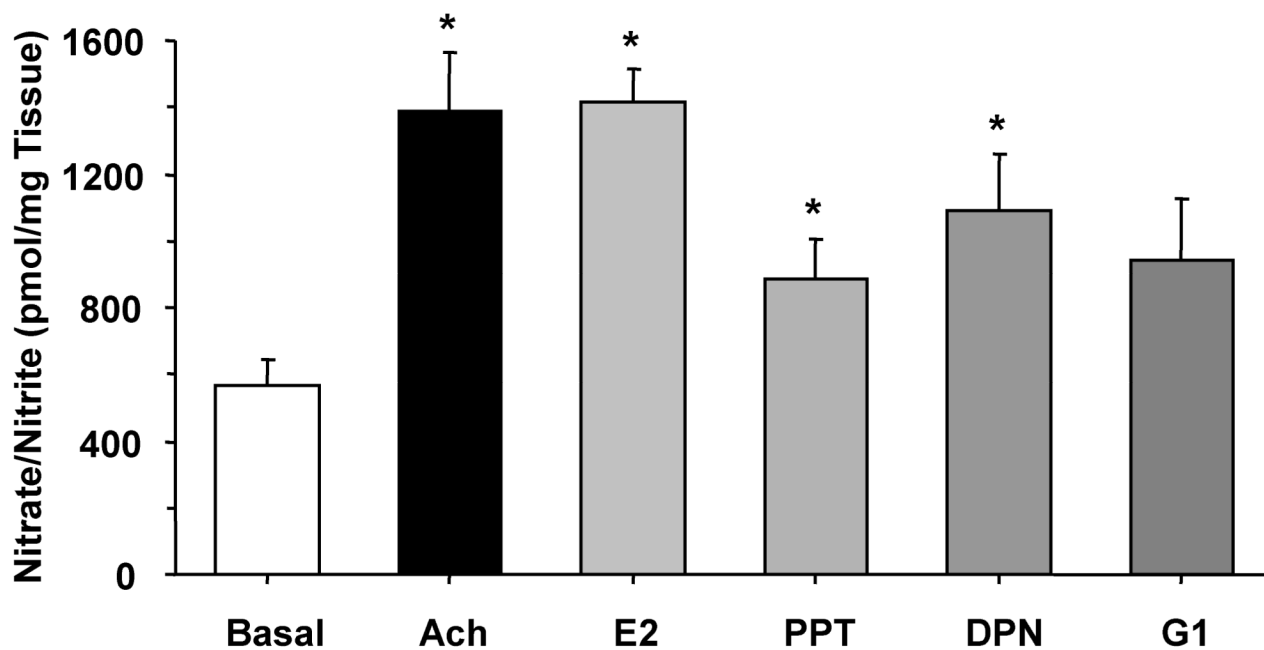


**Fig. 10.** Nitrite/nitrate (NO<sub>x</sub>) production in thoracic aorta of female rat. Aortic rings were incubated in Krebs solution for 30 min and samples were taken for measurement of basal NO<sub>x</sub> production. The rings were stimulated with ACh, E2, PPT, DPN or G1 ( $10^{-5}$  M) for 10 min, and NO<sub>x</sub> production was measured. Data represent means $\pm$ SEM, n = 8. \* Significantly different ( $p < 0.05$ ) from basal levels.

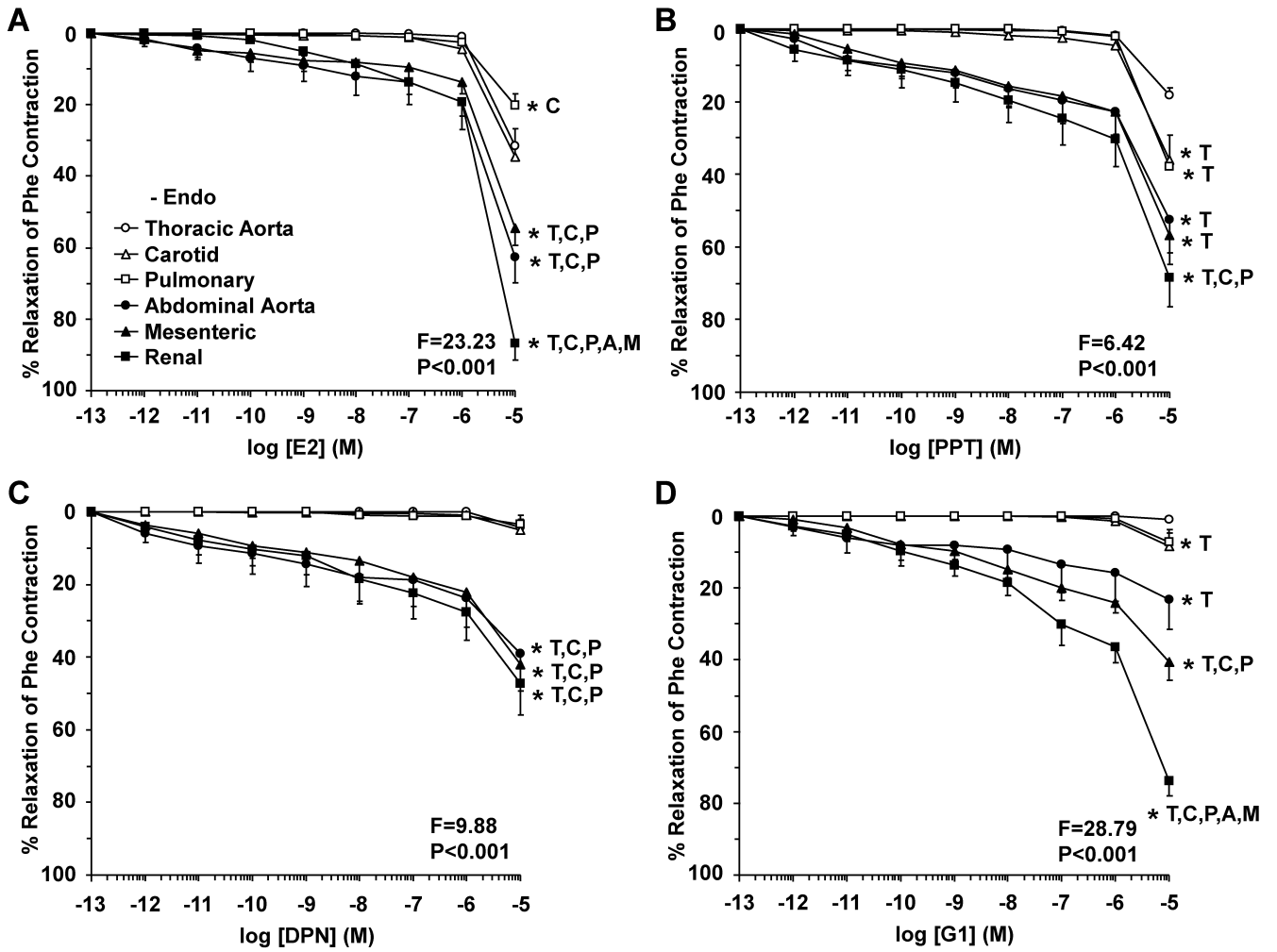


**Fig. 11.** Endothelium-independent ER-mediated relaxation in cephalic, thoracic and abdominal arteries of female rat. Endothelium-denuded segments of thoracic aorta (open circles), carotid (open triangles), pulmonary (open squares), abdominal aorta (closed circles), mesenteric (closed triangles) and renal artery (closed squares) were precontracted with submaximal concentration of Phe then increasing concentrations ( $10^{-12}$  to  $10^{-5}$  M) of  $17\beta$ -estradiol (E2, activator of most ERs) (A), PPT (ER $\alpha$  agonist) (B), DPN (ER $\beta$  agonist) (C), or G1 (GPR30 agonist) (D) were added and the % relaxation of Phe contraction was measured. Data represent means $\pm$ SEM, n= 8 to 10. \* Significantly different (p<0.05) from corresponding measurement in thoracic aorta [T], carotid [C], pulmonary [P], abdominal aorta [A], mesenteric [M] and renal artery [R].

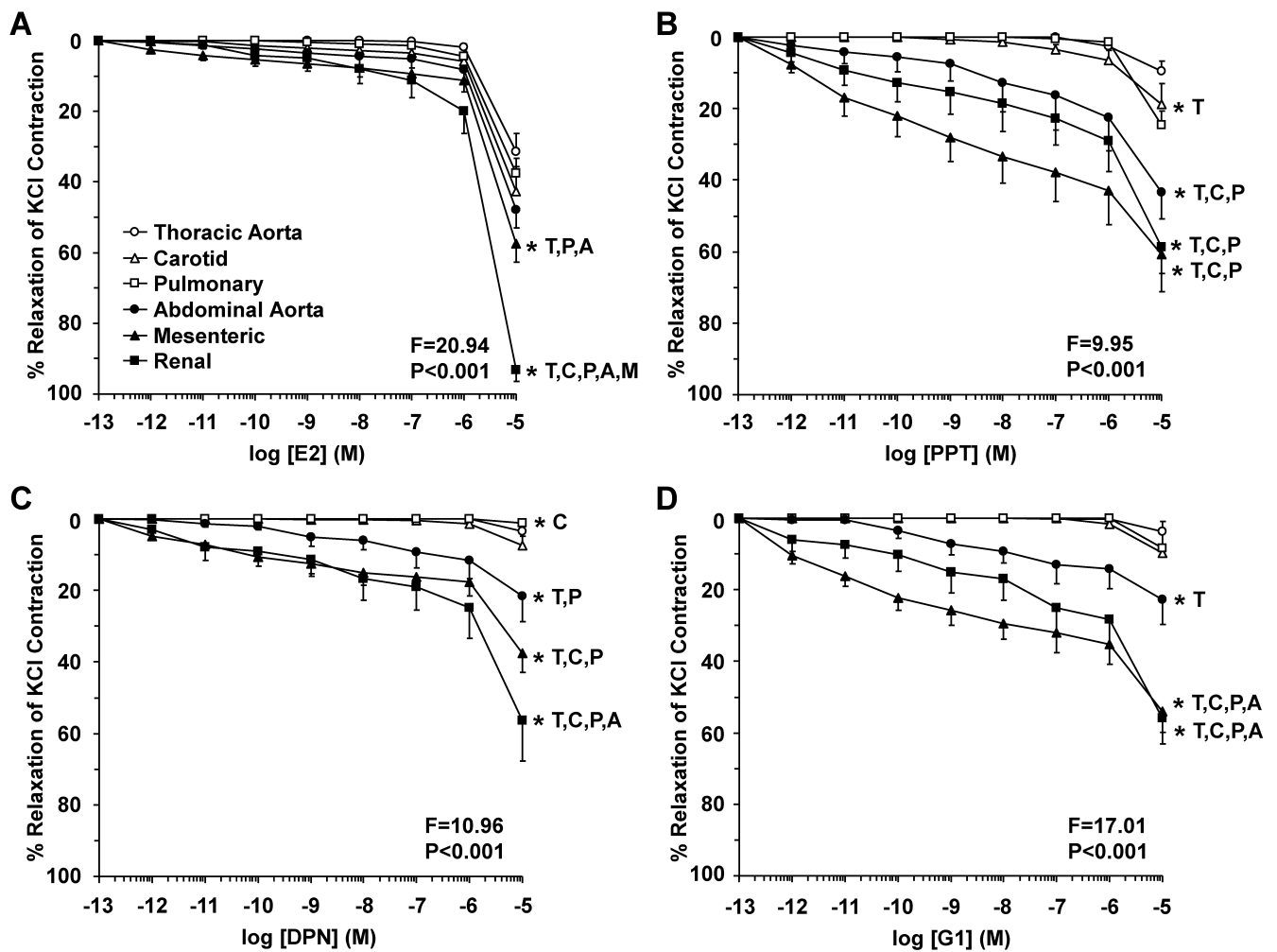


**Fig. 12.** ER-mediated inhibition of Ca<sup>2+</sup>-dependent contraction in cephalic, thoracic and abdominal arteries of female rat. Endothelium-denuded segments of thoracic aorta (open circles), carotid (open triangles), pulmonary (open squares), abdominal aorta (closed circles), mesenteric (closed triangles) and renal artery (closed squares) were stimulated with high KCl (96 mM) depolarizing solution to induce a Ca<sup>2+</sup>-dependent contractile response in VSM. Increasing concentrations (10<sup>-12</sup> to 10<sup>-5</sup> M) of 17β-estradiol (E2, activator of most ERs) (A), PPT (ERα agonist) (B), DPN (ERβ agonist) (C), or G1 (GPR30 agonist) (D) were added and the % relaxation of KCl contraction was measured. Data represent means±SEM, n= 8 to 10. \* Significantly different (p<0.05) from corresponding measurement in thoracic aorta [T], carotid [C], pulmonary [P], abdominal aorta [A], mesenteric [M] and renal artery [R].

EC50 for Phe contraction, ACh relaxation, and ER agonist-induced relaxation in cephalic, thoracic and abdominal arteries of female rat

Table 1

Parameter	Thoracic Aorta	Carotid	Pulmonary	Abdominal Aorta	Mesenteric	Renal
<b>pEC50 (-log M) Phe Contraction</b>						
+ Endo	7.74±0.06	7.81±0.06	8.03±0.04 <sup>*T,C</sup>	7.43±0.05 <sup>*T,C,P</sup>	6.59±0.08 <sup>*T,C,P,A</sup>	6.99±0.07 <sup>*T,C,P,A,M</sup>
- Endo	8.14±0.08 <sup>#</sup>	7.93±0.09	8.11±0.12	7.74±0.06 <sup>#</sup>	6.33±0.14	7.07±0.14
<b>pEC50 (-log M) Relaxation of Phe Contraction ACh</b>						
E2	6.33±0.05	5.56±0.37	6.29±0.07	6.12±0.19	5.75±0.46	6.31±0.15
-Endo	6.72±1.10	2.55±0.38 <sup>*T</sup>	3.44±0.97 <sup>*T</sup>	5.39±0.59 <sup>*C</sup>	4.08±0.56 <sup>*T,C</sup>	5.71±0.40 <sup>*C,p,am</sup>
PPT	2.03±0.20 <sup>#</sup>	3.28±0.56	3.15±0.51	3.85±0.65 <sup>*T</sup>	4.91±0.69 <sup>*‡</sup>	4.51±0.45 <sup>*‡</sup>
-Endo	6.86±0.89	3.65±0.62 <sup>*T</sup>	4.29±0.78 <sup>*T</sup>	6.06±0.60 <sup>*C</sup>	5.46±1.08	5.96±0.28 <sup>*C</sup>
DPN	3.23±0.51 <sup>#</sup>	3.37±0.50	2.28±0.28 <sup>#</sup>	4.96±0.92 <sup>*‡</sup>	5.66±0.88 <sup>*T,C,P</sup>	5.69±0.65 <sup>*T,C,P</sup>
-Endo	7.64±1.33	6.52±1.54	3.45±0.85 <sup>*T</sup>	6.33±0.35 <sup>*‡</sup>	5.77±0.85	5.95±0.85
G1	1.76±0.00 <sup>#</sup>	4.19±1.54	4.73±2.97	7.14±1.34 <sup>*T</sup>	5.68±0.72 <sup>*T,C</sup>	7.01±0.89 <sup>*‡</sup>
-Endo	7.71±1.89	7.15±1.30	4.75±1.55	4.64±0.99	8.26±1.16	5.35±0.82
	1.76±0.00 <sup>#</sup>	3.53±1.03	2.63±0.73	7.56±1.13 <sup>*T,C,P</sup>	7.30±0.40 <sup>*T,C,P</sup>	6.23±0.34 <sup>*T,P</sup>
<b>pEC50 (-log M) Relaxation of KCl Contraction</b>						
E2	2.54±0.40	3.57±0.52	3.18±0.49	3.52±0.78	4.11±0.84	4.07±0.56
PPT	3.09±0.66	4.96±0.66	2.50±0.50 <sup>*C</sup>	5.36±0.84 <sup>*T,P</sup>	8.90±0.62 <sup>*T,C,P,A</sup>	6.68±1.07 <sup>*T,P</sup>
DPN	1.76±0.00	4.01±0.73 <sup>*T</sup>	1.76±0.00 <sup>*C</sup>	5.67±1.16 <sup>*T,P</sup>	5.97±0.98 <sup>*T,P</sup>	5.09±0.90 <sup>*‡,p</sup>
G1	3.50±1.74	3.91±0.89	1.76±0.00	6.56±1.22 <sup>*‡</sup>	8.64±0.75 <sup>*C,P</sup>	6.27±1.15 <sup>*‡</sup>

Data represent means±SEM, n= 8 to 10.

\* Significantly different (p<0.05) from corresponding measurement in thoracic aorta [T], carotid [C], pulmonary [P], abdominal aorta [A], mesenteric [M] and renal artery [R].

# Measurements in endothelium-denuded vessels (-Endo) are significantly different (p<0.05) from corresponding measurements in intact vessels.